


## RESEARCH ARTICLE

# Beneficial effects of CHF6467, a modified human nerve growth factor, in experimental neonatal hypoxic–ischaemic encephalopathy

Elisa Landucci<sup>1</sup> | Dalila Mango<sup>2,3</sup> | Silvia Carloni<sup>4</sup> | Costanza Mazzantini<sup>1</sup> |  
Domenico E. Pellegrini-Giampietro<sup>1</sup> | Amira Saidi<sup>2</sup> | Walter Balduini<sup>4</sup> |  
Elisa Schiavi<sup>5</sup> | Laura Tigli<sup>5</sup> | Barbara Pioselli<sup>5</sup> | Bruno P. Imbimbo<sup>5</sup> |  
Fabrizio Facchinetti<sup>5</sup> 

<sup>1</sup>Department of Health Sciences, Section of Clinical Pharmacology and Oncology, University of Florence, Florence, Italy

<sup>2</sup>Laboratory Pharmacology of Synaptic Plasticity, European Brain Research Institute, Rome, Italy

<sup>3</sup>School of Pharmacy, University of Rome “Tor Vergata”, Rome, Italy

<sup>4</sup>Department of Biomolecular Sciences, University of Urbino Carlo Bo, Urbino, Italy

<sup>5</sup>Corporate Preclinical R&D, Chiesi Farmaceutici, Parma, Italy

## Correspondence

Fabrizio Facchinetti, Corporate Preclinical R&D, Chiesi Farmaceutici, Largo Belloli 11/A, Parma 43122, Italy.  
Email: [f.facchinetti@chiesi.com](mailto:f.facchinetti@chiesi.com)

## Funding information

This study was supported by Chiesi Farmaceutici, Parma, Italy.

## Abstract

**Background and Purpose:** Therapeutic hypothermia (TH) has become the standard care to reduce morbidity and mortality in neonates affected by moderate-to-severe hypoxic–ischaemic encephalopathy (HIE). Despite the use of TH for HIE, the incidence of mortality and disabilities remains high.

**Experimental Approach:** Nerve growth factor (NGF) is a potent neurotrophin, but clinical use is limited by its pain eliciting effects. CHF6467 is a recombinant modified form of human NGF devoid of algogenic activity (painless NGF).

**Key Results:** In rodent hippocampal slices exposed to oxygen and glucose deprivation, CHF6467 protected neurons from death and reverted neurotransmission impairment when combined with hypothermia. In a model of rat neonatal HIE, intranasal CHF6467 (20  $\mu\text{g kg}^{-1}$ ) significantly reduced brain infarct volume versus vehicle when delivered 10 min or 3 h after the insult. CHF6467 (20 and 40  $\mu\text{g kg}^{-1}$ , i.n.), significantly decreased brain infarct volume to a similar extent to TH and when combined, showed a synergistic neuroprotective effect. CHF6467 (20  $\mu\text{g kg}^{-1}$ , i.n.) per se and in combination with hypothermia reversed locomotor coordination impairment (Rotarod test) and memory deficits (Y-maze and novel object recognition test) in the neonatal HIE rat model. Intranasal administration of CHF6467 resulted in meaningful concentrations in the brain, blunted HIE-induced mRNA elevation of brain neuroinflammatory markers and, when combined to TH, significantly counteracted the increase in plasma levels of neurofilament light chain, a peripheral marker of neuroaxonal damage.

**Conclusion and Implications:** CHF6467 administered intranasally is a promising therapy, in combination with TH, for the treatment of HIE.

## KEYWORDS

hypothermia, neonatal brain damage, neuroinflammation, neuroprotection, painless mutant human nerve growth factor

**Abbreviations:** aCSF, artificial cerebrospinal fluid; BBB, blood–brain barrier; CA1, Cornu Ammonis-1; EPSC, excitatory postsynaptic current; FEPSP, field excitatory postsynaptic potential; GD, glucose deprivation; HI, hypoxia–ischaemia; HIE, hypoxic–ischaemic encephalopathy; hNGFp, painless human nerve growth factor; IBs, inclusion bodies; iei, inter-event interval; NFL, neurofilament light; OGD, oxygen and glucose deprivation; PI, propidium iodide; PND, post-natal day; RT, room temperature; sEPSC, spontaneous excitatory postsynaptic current; SPHP, SP Sepharose High Performance; STIC, salt tolerant interaction chromatography; TH, therapeutic hypothermia; TTC staining, triphenyl tetrazolium chloride staining; 18 s rRNA, 18S ribosomal RNA.

## 1 | INTRODUCTION

Neonatal hypoxic–ischaemic encephalopathy (HIE) is the most common cause of death and disability in infants and is often associated with persistent motor, sensory and cognitive impairment (Millar et al., 2017). Brain damage following hypoxic–ischaemic insult is a complex process with multiple contributing mechanisms and pathways resulting in both early and delayed injury (Patel et al., 2014).

Although therapeutic hypothermia (TH) is becoming standard clinical care to reduce morbidity and mortality, it is more effective against moderate than severe HIE (Sabir et al., 2012) with almost 50% of the patients developing adverse outcomes despite cooling. Thus, any preclinical study for evaluating new drugs in HIE, aiming to be translated into future clinical studies, should consider a comparison as well as a combination with TH to assess the potential for additive effects (Landucci et al., 2022).

Nerve growth factor (NGF) is a 120-amino acid protein primarily involved in the regulation of the growth, maintenance, proliferation and survival of cholinergic neurons and in homeostasis of glial cells (Lorenzini et al., 2021). NGF also activates nociceptive neurons to transmit pain signals from the peripheral to the central nervous system (Wise et al., 2021). Although exogenous NGF has been proposed for the treatment of different kinds of peripheral neuropathies (Apfel et al., 1998) and neurodegenerative diseases (Jönhagen et al., 1998), its nociceptive effects limit its clinical use because of the induction of hyperalgesia and allodynia. NGF is produced by astrocytes and microglia, and its expression is markedly upregulated by local tissue damage (Pöyhönen et al., 2019). Intracerebroventricularly administered NGF has been shown to be neuroprotective in an animal model of neonatal HIE (Holtzman et al., 1996). Beside protecting neurons expressing neurotropic receptor tyrosine kinase 1 (TrkA) from a variety of insults (Holtzman et al., 1995), several studies have indicated that NGF has neuroprotective actions that extend beyond neuronal cells, as it can inhibit pro-inflammatory cytokine release and increase the anti-inflammatory ones (e.g., IL-10) (Fodelianaki et al., 2019; Minnone et al., 2017). Because of its high molecular weight, NGF does not readily cross the blood–brain barrier (BBB), thus making challenging the use of NGF as a treatment for central nervous system diseases. A valid alternative approach, which bypasses the BBB, appears to be the intranasal administration and recent studies showed that a significant amount of NGF can reach the central nervous system through this administration route (Capsoni et al., 2017; Li et al., 2018; Manni et al., 2021). The olfactory route seems to be a viable option, as it is relatively simple, not invasive, safe and less likely to cause systemic side effects.

To exploit the neuroprotective potential of NGF while improving its therapeutic window by reducing the known algogenic side effects, a recombinant mutated form of human NGF, namely, CHF6467, also known as ‘painless human NGF’ (hNGFp), has been developed based on the clinical observation that a rare genetic syndrome (hereditary sensory autonomic neuropathy type V) bringing a point mutation on position 100 of NGF (R100W) generates normal phenotype with markedly reduced nociception (Testa et al., 2019). CHF6467 presents

### What is already known?

- Therapeutic hypothermia (TH) is used in neonates affected by hypoxic–ischaemic encephalopathy (HIE)
- However, despite use of TH, mortality and long-term disabilities remain high.

### What does this study add?

- CHF6467, a painless mutant human nerve growth factor, was administered intranasally in experimental neonatal HIE
- CHF6467 is neuroprotective and attenuates neurobehavioural deficits either alone or in combination with TH.

### What is the clinical significance?

CHF6467 (i.n.) is a promising novel therapy, alone or in combination with TH, for HIE.

a mutation on position 100 (R100E) to reduce algogenic activity and another mutation in position 61 (P61S), to analytically distinguish it from the endogenous wild type NGF. Compared to human NGF, CHF6467 exhibits similar affinity for the ‘neurotrophic’ TrkA receptors (1.35 vs. 0.94 nM) while significantly lower affinity for the ‘apoptotic’ p75 receptor (200 vs. 1.53 nM) (Covaceuszach et al., 2010). Functionally, CHF6467 shows identical neurotrophic and neuroprotective properties to the wild-type NGF but with at least 10 times less algogenic activity (Capsoni et al., 2011; Malerba et al., 2015; Severini et al., 2017). Recently, it was observed that intranasal administration of CHF6467 in a mouse model of Alzheimer’s disease differentially modulated microglia and astroglia, by regulating tumour necrosis factor- $\alpha$  (TNF- $\alpha$ ) expression and reducing amyloid- $\beta$  deposits by increasing their clearance (Capsoni et al., 2017).

In the present study, we investigated the hypothesis that intranasal CHF6467 could, either per se or in combination with TH, reduce brain damage and improve behavioural outcomes in rat models of neonatal HIE. We also assessed the ability of CHF6467 to counteract HIE-induced gene expression of neuroinflammatory mediators and plasma elevation of neurofilament light chain, a recognized biomarker of neuronal damage widely used in the clinic.

## 2 | METHODS

### 2.1 | Animals and ethical approval

Wistar rats, Sprague–Dawley rats and C57BL/6J mice were used in the different experimental protocols. All surgical and experimental procedures were carried out in accordance with the Italian regulations

for the care and use of laboratory animals (EU Directive 2010/63/EU) and were approved by appropriate institutional and state authorities of University of Florence (17E9C.N.GS0., No. 671/2019-PR and No. 22/2022-PR), University of Urbino Carlo Bo (No. 312/20200-PR) and EBRI Rita Levi-Montalcini Foundation (F8BBB.N.ACZ). In compliance to the Italian law and EU directives, all efforts were made to minimize the number of animals used and suffering according to the principle of 3Rs. Animal studies are reported in compliance with the [ARRIVE guidelines](#) (Percie du Sert et al., 2020) and with the recommendations made by the British Journal of Pharmacology (Lilley et al., 2020).

## 2.2 | Preparation of CHF6467 and intranasal administration

For all studies, CHF6467 (hNGFp) was provided by Chiesi Farmaceutici S.p.A. (Parma, Italy) and was produced by recombinant expression in *E. coli* strain BL21 using a 100 L fermentation scale process. The resulting biomass was harvested by centrifugation, and the inclusion bodies (IBs) were released by homogenization, separated by centrifugation and washed. The further processing of the IBs included solubilization, reduction of disulphide bridges and refolding. After refolding, the pro-hNGFp was converted to hNGFp by cleavage of the pro-protein with trypsin. After trypsin cleavage, purification of hNGFp started with a mixed mode cation exchange chromatography, followed by salt tolerant interaction chromatography (STIC) membrane filtration and ultrafiltration and cation exchange chromatography on SP Sepharose High Performance (SPHP) resin. The SPHP pool is diafiltered into the formulation buffer (20 mM Acetic acid, 20 mM L-Methionine, pH 5.5) at target concentration of 2 mg ml<sup>-1</sup> and stored at ≤ -65°C.

Vehicle-treated animals were administered with an equivalent volume of an aqueous solution of 20 mM L-methionine in 20 mM acetate buffer, pH 5.5. A total volume of 4 µl (2 µl per nostril) was administered, alternating nostrils with an interval of 2 min. This intranasal (i.n.) administration protocol was well tolerated with no relevant sign of distress observed in the animals.

## 2.3 | Studies in rat organotypic hippocampal slices exposed to oxygen–glucose deprivation

Male and female Wistar rat pups (7–9 days old) were obtained from Charles River (Milan, Italy). Animals were housed at 23 ± 1°C under a 12 h light–dark cycle (lights on at 07:00) and were fed a standard laboratory diet with ad libitum access to water. Organotypic hippocampal slice cultures were prepared as previously described (Gerace et al., 2012). Briefly, the hippocampi were removed from the brains of 7–8 day old Wistar rats, and transverse slices (420 µm) were prepared using a McIlwain tissue chopper in a sterile environment. Isolated slices were first placed in ice-cold Hanks' balanced salt solution (HBSS), supplemented with 5 mg ml<sup>-1</sup> glucose and 1.5% Fungizone® (GIBCO-BRL) and then transferred to humidified semi-porous membranes (30 mm Millicell-CM 0.4 µm tissue culture plate

inserts, Millipore, Rome, Italy; four per membrane). These were placed in six-well tissue culture plates containing 1.2 ml culture medium containing 50% Eagle's minimum essential medium (MEM), 25% heat-inactivated horse serum, 25% Hanks' balanced salt solution (HBSS), 5 mg ml<sup>-1</sup> glucose, 1 mM glutamine and 1.5% Fungizone®. Slices were maintained at 37°C, with 100% humidity, and 95% air: 5% CO<sub>2</sub> atmosphere, and the medium was changed every 3 days. Experiments were carried out after 14 days in vitro (DIV). Oxygen and glucose deprivation (OGD) was induced as previously described (Landucci et al., 2011, 2021). Briefly, the slices were exposed to a serum-free medium saturated with 95% N<sub>2</sub>/5% CO<sub>2</sub> at 37°C in a gassed incubator equipped with an oxygen controller (BioSpherix, New York, United States). After 30 min, the cultures were transferred to oxygenated serum-free medium containing 5 mg ml<sup>-1</sup> glucose and returned to the incubator under normoxic conditions. Drugs were present in the incubation medium during 30 min OGD period and in subsequent 24 h recovery period. The neuronal injury was evaluated 24 h later. Cell injury was assessed using the fluorescent dye propidium iodide (PI) (5 µg ml<sup>-1</sup>) that was added to the medium at the end of the 24 h post-OGD recovery period. Thirty minutes later, fluorescence was viewed using an inverted fluorescence microscope (Olympus IX-50; Solent Scientific, Segensworth, United Kingdom) equipped with a xenon-arc lamp, a low-power objective (4X) and a rhodamine filter. Images were digitized using a video image obtained with a CCD camera (Diagnostic Instruments Inc., Sterling Heights, MI, United States) controlled by software (InCyt Im1TM; Intracellular Imaging Inc., Cincinnati, OH, United States) and subsequently analysed using the Image-Pro Plus morphometric analysis software (Media Cybernetics, Silver Springs, MD, United States). To quantify cell death, the CA1 hippocampal subfield was identified and encompassed in a frame using the drawing function in the image software (ImageJ; NIH, Bethesda, MD, United States), and the optical density of PI fluorescence was recorded. There was a linear correlation between CA1 PI fluorescence and the number of injured CA1 pyramidal cells.

## 2.4 | Studies in mouse hippocampal slices exposed to oxygen–glucose deprivation

C57BL/6J male mice (15–25 days old) were housed at the EBRI Rita Levi-Montalcini Foundation (Rome, Italy). The mice were killed by cervical dislocation (Clarkson et al., 2022), and the brain was rapidly removed from the skull and immersed in cold aCSF. Parasagittal hippocampal slices (250–350 µm) were obtained according to the standard procedures (Mango & Nisticò, 2019). A single slice was placed in the recording chamber submerged in a continuously flowing solution (3 ml min<sup>-1</sup>) of aCSF saturated with 95%O<sub>2</sub> to 5%CO<sub>2</sub>. Extracellular field recordings were performed at 30 ± 0.5°C using a stimulating electrode placed in Schaffer collateral fibres to elicit fEPSP that was recorded with glass microelectrodes (1.5–2 MΩ) filled with aCSF placed in the CA1 region of the stratum radiatum. Whole cell patch-clamp recordings on CA1 pyramidal neurons were performed at room temperature and held at -70 mV. Whole-cell configuration was

obtained using glass electrodes (4–7 M $\Omega$ ) in voltage-clamp mode filled with solutions containing (in mM) CsCl (135), KCl (10), CaCl<sub>2</sub> (0.05), EGTA (0, 1), Hepes (10), Na<sub>3</sub>-GTP (0, 3), Mg-GTP (4, 0), pH adjusted to 7.3 with CsOH. The OGD on ex vivo hippocampal slice was applied by perfusion with aCSF without glucose and gassed with 95%N<sub>2</sub> to 5% CO<sub>2</sub> (49). After OGD the slices were reperfused with aCSF containing glucose and O<sub>2</sub>. The neuroprotective effect of CHF6467 against OGD was evaluated on the amplitude of field excitatory post synaptic potentials (fEPSPs) and on single neuron parameters altered by energy deprivation; specifically, we measured amplitude and inter event interval (iei) of spontaneous excitatory post synaptic currents (sEPSC) and membrane potential (Vm). We also assessed the time window of neuroprotection with CHF6467 during and after OGD, recording evoked EPSC. All patch clamp experiments have been carried out in presence of picrotoxin to isolate the excitatory neurotransmission.

## 2.5 | Study in neonatal Sprague–Dawley rats subjected to brain hypoxic–ischaemic insult (research site at University of Urbino)

Pregnant Sprague–Dawley rats (Charles River Laboratories, Italy) were housed in individual cages kept in regular light/dark cycle (lights on 8 AM to 8 PM) in the animal facility of the Department of Biomolecular Sciences of the University of Urbino Carlo Bo. The day of delivery was considered Day 0. Pup rats from different litters were randomized and normalized to 10 pups for litter. On post-natal day (PND) 7, pups were anaesthetized with 3% isoflurane in oxygen and the right common carotid artery of each pup was exposed, isolated from nerve and vein and permanently ligated with surgical silk. After suturing the wound, animals recovered for 3 h under a heating lamp. At the end of this procedure, pups were placed in airtight jars partially submerged in a water bath at 37°C to maintain a constant thermal environment and exposed for 2.5 h to a humidified nitrogen–oxygen mixture (92% and 8%, respectively) delivered at 5–6 L min<sup>-1</sup> (hypoxia–ischaemia, HI). Rectal temperatures were measured before surgery and at the end of the period of hypoxia; no differences were found among groups (data not shown). Previous studies have shown that rectal temperature accurately reflects brain temperature in rodents during exposure to HIE (Chen et al., 2024; Dingley et al., 2006). CHF6467 was intranasally administered at the dose of 4  $\mu\text{g kg}^{-1}$  (low dose) 10 min after HI or at the dose of 20  $\mu\text{g kg}^{-1}$  (high dose), 10 min, 1 h or 3 h after the insult according to the manufacturer instructions. A group of ischaemic animals received the same volume of vehicle 10 min after HI (VEH). Animals were then returned to their dams until PND 14 (7 days after HI and CHF6467 treatment), when they were killed to evaluate the neuroprotective effect of CHF6467 using histological techniques. Briefly, animals were anaesthetized with 3% isoflurane in oxygen and euthanized by decapitation, and the brains immediately frozen in dry ice. Coronal sections (40  $\mu\text{m}$  thick) of the brain of each animal were cut on a cryostat and thaw-mounted onto acid-washed subbed slides (gelatin and chrome alum). Sections were then post-fixed with 4% paraformaldehyde in phosphate-buffered saline and

stained with toluidine blue. To evaluate tissue injury, a computerized video camera-based image analysis system (J Image software; <https://imagej.nih.gov/ij>) was used to measure cross-sectional areas from the level of the anterior genu of the corpus callosum to the end of the dentate gyrus (3.0 mm anterior to bregma, –3.0 mm posterior to bregma; figs. 9a and 49a in the König and Klippel rat brain stereotaxic atlas). Measurements were performed in blinded conditions and were based on the intensity and uniformity of the staining of the intact tissue as previously described (Carloni & Balduini, 2008). Regional volumes were estimated by summing areas and multiplying by the distance between sections (400  $\mu\text{m}$ ). Statistical analysis was performed using the computer program Graph Pad Prism (v 8.0, Graph Pad Software Inc., San Diego, CA, United States). Statistical differences between groups for each outcome measured were analysed using one-way ANOVA followed by the Holm-Sidak procedure for multiple comparisons. All the data were expressed as mean  $\pm$  SEM and significance was set at  $P \leq 0.05$ .

## 2.6 | Studies in neonatal Wistar rats subjected to brain hypoxic–ischaemic insult with or without therapeutic hypothermia (TH) (research site at University of Florence)

Pregnant Wistar rats (Charles River Laboratories, Italy) were housed in individual cages in the animal facility of the University of Florence and kept in regular light/dark cycle (lights on 8 AM to 8 PM). The day of delivery was considered Day 0. Pup rats from different litters were randomized and normalized to 10 pups for litter. Brain hypoxic–ischaemic insult was obtained as previously described (Landucci et al., 2018). Briefly, at PND 7, Wistar rat pups were anaesthetized with isoflurane gas (induction, 4–5%; maintenance, 1–2%). The left common carotid artery was permanently ligated using 4–0 silk following a midline incision. After the operation, all pups were returned to their dams for recovery and lactation for 1 h. Then, pups were placed in enclosed, vented Plexiglas chambers (W20, D20 and H17) partially submerged in a water-bath and exposed by continuous flow to warmed, humidified gas 8% oxygen 92% nitrogen for 120 min.

After the insult, the pups were returned to their dams for 1 h and then placed in a chamber at normothermic (37°C) or hypothermic (32°C) temperatures for 4 h.

Pups dedicated to assessment of infarct volume 72 h after the insult were administered with CHF6467 (20 and 40  $\mu\text{g kg}^{-1}$  i.n.) immediately and 24 h after the end of hypoxia. All pups were then maintained with their dam and killed by decapitation 72 h later. For the measurement of the infarct (ischaemic) areas and volumes, 1 mm thick coronal sections were cut with a blade, incubated in 2% 2,3,5-triphenyl-tetrazolium chloride (TTC) for 15 min at 37°C and then fixed in 4% paraformaldehyde for 24 h. Infarct areas were measured using a computerized image analysis system (Image-Pro Plus 3.0). The infarct volume was calculated as previously described (Landucci et al., 2018).

Pups dedicated to neurobehavioural testing were administered with CHF6467 (20  $\mu\text{g kg}^{-1}$ ) by intranasal immediately and 24, 48 and

72 h after the end of hypoxia were then maintained with their dam until weaning, and they were subjected to behavioural tests at PND 60.

## 2.7 | Behavioural tests at PND 60 (research site at University of Florence)

Open field test, Novel object recognition, RotaRod and Y-maze have been performed at PND 60 for evaluating long-term neurological function.

## 2.8 | Novel object recognition test

The novel object recognition test evaluates memory on rats. Rats were placed near the centre of the front wall with their back towards the objects for 5 min in an arena to perform the recognition task of two objects with the same colour, size, shape and relatively heavy to prevent animals from moving them around. Interaction with such objects in this first test was employed to ensure that there would be no intrinsic preferences or aversions and that each object would be equally explored, for similar durations (habituation phase). For the assessment of short-term memory (Vogel-Ciernia & Wood, 2014), the animals were placed again in the open field arena at 30 min from habituation, in the presence of two objects, one of them being novel to the animal (with different shape and size from the other familiar object). The act of directing the nose to the object at a distance inferior to 2 cm and/or touching the object with the nose or mouth was considered as exploration. Each session was videotaped for 5 min and then analysed. The evaluated parameters were interaction time with the novel object (in seconds), interaction time with the familiar object (in seconds) and the discrimination index, calculated as the difference in the exploration time for the novel object (N) compared to the familiar (F) one as a proportion of the total time spent exploring the two objects  $(N - F) / (N + F)$ .

## 2.9 | RotaRod

The RotaRod test evaluates equilibrium behaviour and locomotor ability in rodents. At 60 post-natal days, the effect of combined treatment was evaluated by RotaRod tests. The RotaRod apparatus (Ugo Basile, Varese, Italy) consisted of a base platform and a rotating rod with a diameter of 6 cm and a non-slippery surface. The rod was placed at a height of 25 cm from the base. The rod, 36 cm in length, was divided into four equal sections by five disks. The day before the test, animals were trained to perform the task. They were placed on the rod with no rotation for 30 s, then with a constant rotation (10 rpm), and this procedure was repeated three times at 10 min intervals. Animals were trained until they could stay on the rod for at least 4 falls. After 24 h in the testing session, animals were placed on the rod for the testing trial, in which the rod rotates with the same constant speed (Manni, Leotta, et al., 2023). The integrity of motor

coordination was assessed based on the number of falls from the rod for a maximum of 360 s. After a maximum of four falls from the rod, the test was suspended, and the time was recorded. Each rat was assessed once, and the group mean average score was calculated. Rodents with impaired locomotor function fall from the rod faster than those with normal locomotor function.

## 2.10 | Y-maze

The Y-maze is commonly used to assess spontaneous alternation and spatial memory in rodents. It consists of three arms with 120° angle between each other. The Y-maze was initially used to study exploration behaviour and behaviour pattern (known as spontaneous alternation), and for assess spatial memory in rodents by evaluating spontaneous alternation. This test includes a single trial, in which the animal is placed in one arm of the Y-maze and allowed to explore for 5 min. The sequence of each entrance and total number of entrances are recorded. Spontaneous alternation is shown by the tendency of the arm visits that are different from previous two visits.

After the end of the behavioural experiments at 60 PND, rats were perfused transcardially with an ice-cold solution of 4% paraformaldehyde in PBS. Brains were extracted, postfixed overnight at 4°C with a solution of 4% paraformaldehyde in PBS and cryoprotected with a solution of 18% sucrose in PBS for at least 48 h. A collection of coronal sections (20 µm thick) of the brains has been carried out using a microtome cryostat (CM1850; Leica, Nussloch, Germany) and stained with toluidine blue. All sections were scanned to the computer using the Axio system (Z1 system; Zeiss, Germany). The area of brain damage was measured using image-analysis system (NIH ImageJ software, <https://imagej.nih.gov/ij>). The infarct volume was estimated with the direct method by summing areas of the selected slices where the damage is present and multiplying by the distance between sections (400 µm). Statistical differences between groups for each outcome measured were analysed using two-way ANOVA followed by Tukey's post hoc. All the data were expressed as mean ± SEM, and significance was set at  $P \leq 0.05$ . All statistical analyses were performed using GraphPad Prism 8.0 (Graph Pad Software Inc., San Diego, CA, United States).

## 2.11 | Study on neonatal Wistar rat brain cytokines and chemokines subjected to brain hypoxic-ischaemic insult

Wistar rats at PND 7 were subjected to brain hypoxic-ischaemic lesion as described in the previous paragraph. CHF6467 was administered intranasally only immediately after the end of hypoxia at the doses of 20 µg kg<sup>-1</sup>. All the pups were then maintained with their dam and killed by decapitation 24 h later. The brain was immediately extracted from the skull, and cortex and hippocampus were rapidly dissected on a cold plate kept on ice, rinsed in cold PBS and immediately lysed with QIAzol Lysis Reagent (0.8 ml per 30 mg tissue).

Tissue samples were homogenized combining beads and Tissue Lyser (Qiagen, Hilden, Germany) device. After addition of chloroform, the homogenate was separated into aqueous and organic phases by centrifugation. The upper, aqueous phase was extracted by QiaCube system (Qiagen, Hilden, Germany). Protocol including DNase step was chosen in order to remove gDNA. RNA samples were eluted in RNase free water and stored at  $-80^{\circ}\text{C}$  until Reverse transcription step. Concentration of RNA samples was determined by Nanodrop (ThermoFisher, Frosinone, Italy) analyser and adjusted to retrotranscribe 1,000 ng of RNA in one RT reaction for each sample. An additional ezDNase™ Enzyme step was performed before RT reaction in order to remove gDNA. Thermal cycling conditions suggested by the manufacturer were followed to allow RT reaction. cDNA samples were tested on custom designed array plates (Taqman gene array, ThermoFisher) including primers and probe for target and housekeeping genes. The following genes (ThermoFisher, Frosinone, Italy, catalogue number in brackets) were targeted during the study: Housekeeping genes: 18 s rRNA (Hs9999901\_s1), Beta-2-microglobulin (B2m) (Rn00560865\_m1), TATA box-binding protein (Tbp) (Rn01455648\_m1); Target genes: monocyte chemoattractant protein-1 (Ccl2) (Rn00580555\_m1), chemokine ligand 22 (Ccl22) (Rn01536591\_m1), chemokine ligand 112 (Ccl12) (Rn01464638\_m1), Tnf (Rn00562055\_m1), Cxcl2 (Rn00586403\_m1), Ccl7 (Rn01467286\_m1), CC-chemokine receptor 5 (Ccr5) (Rn02132969\_s1), chemokine ligand 20 (Ccl20) (Rn00570287\_m1), Il6 (Rn01410330\_m1), Cxcl10 (Rn01413889\_g1), and monocyte chemoattractant protein-6 (Ccl6) (Rn01456400\_m1). TaqMan® Fast Advanced Master Mix (Applied Biosystems, Monza, Italy) and diluted cDNA were added to plates; thermal cycling conditions suggested by manufacturer were followed to carry out PCR reaction. Results were calculated using the  $2^{-\Delta\Delta\text{Ct}}$  method based on housekeeping gene amplification. Statistical analysis was performed by Graph Prism 8.0 software; one-way ordinary ANOVA test followed by Dunnett post hoc test.

## 2.12 | Study on neurofilament light chain plasma levels in neonatal rats subjected to hypoxic–ischaemic encephalopathy (HIE)

At PND7, Wistar rats subjected to hypoxic–ischaemic insult were treated with intranasal CHF6467 ( $40\ \mu\text{g}\ \text{kg}^{-1}$ ) or hypothermia or their combination as described in the previous paragraphs. In a subset of animals at PND 10, three days after the insult, plasma samples were collected, immediately upon killing. NfL plasma levels were measured by Rat NfL Simple Plex assay on Ella device (ProteinSimple, California, United States), according to the manufacturer's instructions.

## 2.13 | Data and statistical analysis

The data and statistical analysis comply with [the recommendations of the British Journal of Pharmacology on experimental design and analysis in pharmacology](#) (Curtis et al., 2022).

Operators blinded to the experimental group allocation performed statistical analysis for neuroprotective experiments, electrophysiological experiments, behavioural tests, cytokines and NfL dosages. Statistical analyses were performed using GraphPad Prism 8 (GraphPad Software). Statistical analysis was performed without taking sex into account for assignment to experimental groups, because preliminary analyses for the effects of both HIE and intranasal CHF6467 on males and females did not reveal a main or interaction effect related to sex. The Shapiro–Wilk normality test was used to determine if variables followed a normal distribution. Results are presented as means  $\pm$  SEM (for data with Gaussian distribution) or median  $\pm$  range (for data with non-Gaussian distribution). Statistical comparisons of data obtained from electrophysiological experiments were performed using the Student's *t* test (unpaired data) or with one-way ANOVA followed by Bonferroni's post hoc test. In OGD experiments, significance was evaluated in the last 10 min of recordings, and statistical significance was set at  $P < 0.05$ . Amplitude or inter-event interval of the spontaneous events was detected from 3 min trace records, and changes were compared according to their cumulative distributions using the Kolmogorov–Smirnov (K-S) test.

Statistical differences between groups for SD rats were analysed using one-way ANOVA followed by the Holm–Sidak procedure for multiple comparisons.

To assess effects of HIE and CHF6467 treatment alone or in combination with hypothermia (in Wistar rats) on the neuroprotection and behavioural tests, one-way ANOVA was performed, followed by Tukey's *w* test for multiple comparisons. Statistical comparisons of data obtained from cytokines and NfL dosages were analysed using one-way ANOVA was performed, followed by Dunnett's test for multiple comparisons. Post-hoc tests were run only if *F* achieved  $P < 0.05$  and there was no significant variance inhomogeneity.

## 2.14 | Nomenclature of targets and Ligands

Key protein targets and ligands in this article are hyperlinked to corresponding entries in the IUPHAR/BPS Guide to PHARMACOLOGY <http://www.guidetopharmacology.org> and are permanently archived in the Concise Guide to PHARMACOLOGY 2023/23 (Alexander et al., 2023).

## 3 | RESULTS

### 3.1 | CHF6467 attenuates oxygen and glucose deprivation (OGD)-mediated injury in rat organotypic hippocampal slices

We investigated the effects of CHF6467 on CA1 toxicity induced by OGD in rat organotypic hippocampal slices (Figure 1a). In basal conditions, rat organotypic hippocampal slices exposed to CHF6467 ( $0.001\text{--}1\ \mu\text{g}\ \text{ml}^{-1}$ ) for 24 h displayed no apparent signs of injury (data not shown). When present in the incubation medium during OGD and

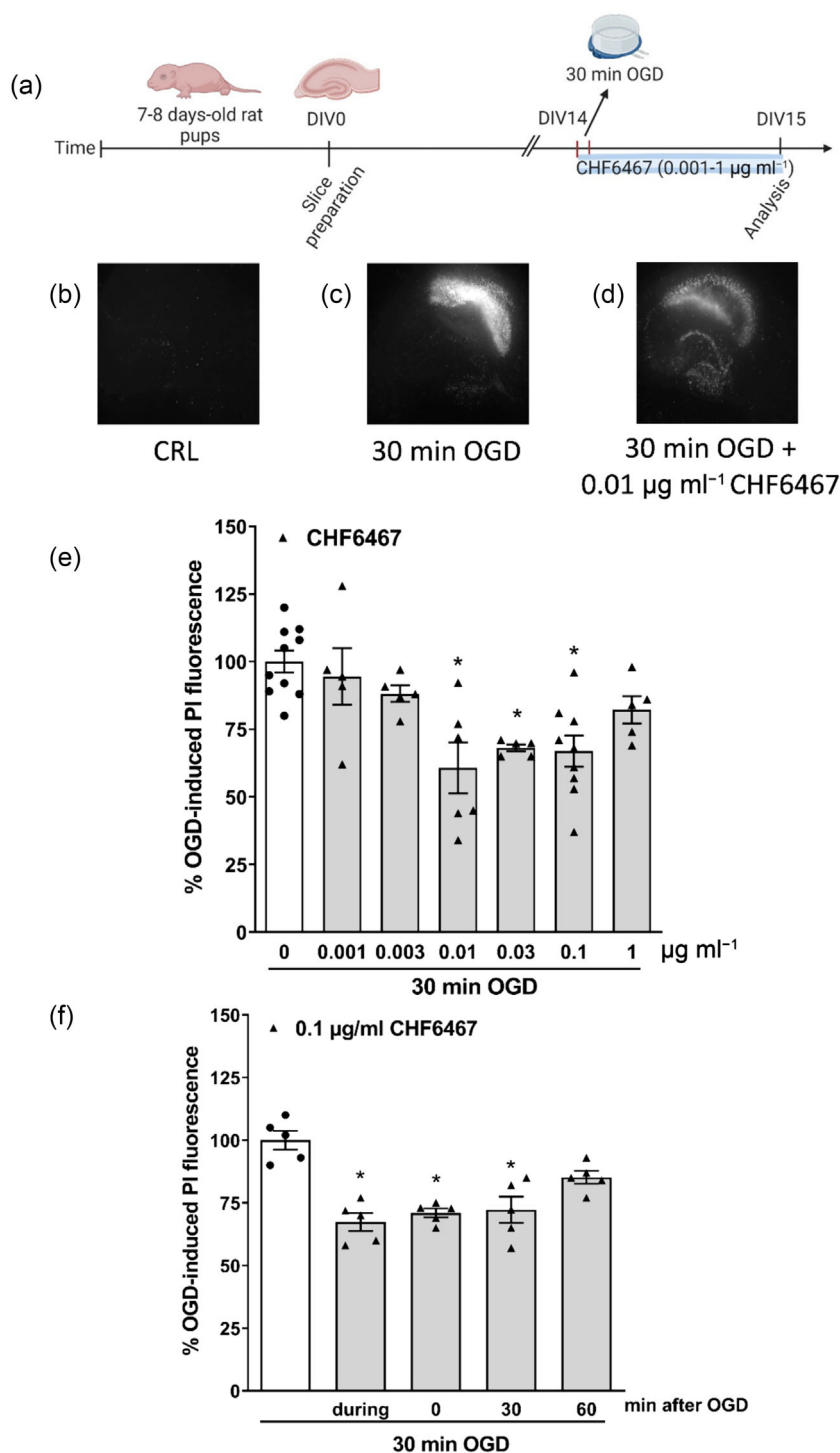


**FIGURE 1** Neuroprotective effects of CHF6467 against 30 min oxygen and glucose deprivation (OGD) in organotypic hippocampal slices. (a) Schematics of experimental timeline used for the study of hippocampal organotypic slices under ischaemic condition (see Section 2). DIV: day in vitro. (b) Hippocampal slice under control conditions (CRL) (background propidium iodide (PI) fluorescence). (c) Slice exposed to 30 min OGD displaying intense PI labelling in the CA1. (d) CA1 damage induced by 30 min OGD was attenuated by the presence of 0.01 µg ml<sup>-1</sup> of CHF6467. (e) CHF6467 dose-dependently attenuated CA1 injury. (f) CHF6467 showed neuroprotective effects at different time points after 30 min OGD in organotypic hippocampal slices. Data are expressed as mean ± SEM of at least five experiments run in quadruplicate. \**P* < 0.05 versus OGD; one-way ANOVA followed by Dunnett's test

in the subsequent 24 h of recovery period, CHF6467 reduced the CA1 injury, the maximum protection being achieved at 0.01–0.1 µg ml<sup>-1</sup> (Figure 1b–e). To investigate the time therapeutic window, rat organotypic hippocampal slices were subjected to 30 min OGD and treated with CHF6467 (0.1 µg ml<sup>-1</sup>) at different time points (0, 30 and 60 min) after the insult. Figure 1f shows that the protective effects of CHF6467 were still manifest when the drug was administered up to 30 min following OGD.

### 3.2 | CHF6467 reverts oxygen and glucose deprivation (OGD)-mediated synaptic depression in acute mouse hippocampal slices

We investigated the effects of CHF6467 on electrophysiological activity of acute mouse hippocampal slices obtained from mice P15–25 representing early post-natal period (Brust et al., 2015). First, we evaluated the effects of increasing CHF6467

concentrations ( $0.01\text{--}0.1\ \mu\text{g ml}^{-1}$ ) on basal neurotransmission in hippocampus. Bath application of CHF6467 for 15 min at the concentration of  $0.1\ \mu\text{g ml}^{-1}$  affected neurotransmission by inducing a significant increase of fEPSP amplitude compared to control condition (Figure 2a). No significant effects were observed at lower CHF6467 concentrations. Second, we investigated the possibility of neuroprotective effect of CHF6467 against OGD insult. The ability of hippocampal slices to recover synaptic function upon return of normal oxygenation depends on the duration of the OGD (Armogida et al., 2011). OGD applied for 5 min caused a reversible fEPSP depression that reverted on return of normal oxygenated artificial cerebrospinal fluid (aCSF) with glucose (Figure S1a). Conversely, application of OGD for 10 min induced an irreversible fEPSP depression (Figure S1a). To assess neuroprotection, slices were treated with CHF6467 at  $0.03$  or  $0.1\ \mu\text{g ml}^{-1}$  during OGD. At both concentrations, we observed a complete recovery of fEPSP amplitude to control condition (Figure 2b). Next step was to test whether CHF6467 may also prevent the synaptic transmission alteration induced by a prolonged period of glucose deprivation (GD). Under this condition, no neuroprotection was observed with CHF6467 (Figure S1b). Then, we studied the time window of neuroprotection performing experiments in which CHF6467 ( $0.03\ \mu\text{g ml}^{-1}$ ) was applied 5 min after the start OGD perfusion. Surprisingly, also in these conditions, we observed a neuroprotective effect of CHF6467, with a completely restored fEPSP amplitude (Figure 2c). To evaluate the therapeutic window of the observed neuroprotective effect, we performed experiments on hippocampal pyramidal neurons using whole cell patch clamp configuration. The evoked excitatory postsynaptic currents (EPSCs) were irreversibly reduced after 15 min of OGD, but we observed a neuroprotective effect of CHF6467 when it was applied after OGD with a reduction of EPSC depression magnitude induced by OGD (Figure 2d). No EPSC changes were observed when CHF6467 was applied under normal conditions (Figure S1c). When CHF6467 was bath applied 10 min after OGD, we still observed a complete rescue of EPSC reduction induced by OGD (Figure 2e).

### 3.3 | CHF6467 plus hypothermia reverts oxygen and glucose deprivation (OGD)-mediated electrophysiological alterations in mouse hippocampal pyramidal neurons

We evaluated the neuroprotective effects of CHF6467 and hypothermia on electrophysiological parameters altered by energy deprivation on single CA1 pyramidal neuron. We ascertained excitatory neurotransmission measuring spontaneous postsynaptic currents (sEPSC) and membrane potential (Vm). During OGD, we observed a significant reduction in the inter-event interval (iei) of sEPSCs (Figure 3a,b), this effect being linked to the increased glutamate release underlying the excitotoxic mechanism induced by OGD (Castillo et al., 1996). The inter-event interval decrease induced by OGD was reverted by re-oxygenation (Figure 3a,b), while no change was observed in the

amplitude of the same currents during OGD (Figure 3a,b) and after reoxygenation (Figure 3a,b). Notably, perfusion of CHF6467 ( $0.03\ \mu\text{g ml}^{-1}$ ) during the OGD period significantly reversed the effect of OGD on the reduction of iei of sEPSC (Figure 3a,b). A significant effect was also observed during the reoxygenation period in neurons treated with CHF6467, in which we recorded a strong increase of iei compared to reoxygenation alone (Figure 3a,b). No changes were observed in the amplitude of the same events in different conditions (Figure 3a,b), as well as no changes in the same parameters were caused by CHF6467 under normal conditions (Figure S1d). These data show that CHF6467 was able to reduce excitotoxicity induced by OGD. Another parameter that is classically affected by OGD is the membrane potential (Vm). During OGD, the neuron depolarizes and returns to control values during reoxygenation (Figure 3c). In neurons perfused with CHF6467, we did not observe any significant change in the Vm during the OGD period (Figure 3c), while the hyperpolarization during reoxygenation was increased. These data further confirm a neuroprotective potential of CHF6467. We hypothesized that CHF6467 could enhance the neuroprotective effects of TH, which is the current standard clinical care in neonatal HIE. To investigate such a hypothesis, we performed experiments applying CHF6467 with hypothermia in the OGD model (Öz & Saybaşı, 2017). In our experimental conditions, hypothermia (aCSF  $4^{\circ}\text{C}$  for 15 min) was able to partially revert the reduction of EPSC induced by OGD (Figure 3d). The application of CHF6467 during hypothermia completely rescued the OGD reduction of EPSCs (Figure 3d) suggesting an additive effect of CHF6467 with hypothermia, thus providing a rationale for its use as combined treatment in hypoxic-ischaemic brain injury.

### 3.4 | CHF6467 dose-response and time window of intervention in experimental neonatal rat hypoxic-ischaemic encephalopathy (HIEO)

A first set of experiments conducted at University of Urbino, Italy, evaluated the neuroprotective dose-response effects and the time-window for intervention of CHF6467 administration in neonatal Sprague-Dawley rats undergoing brain hypoxic-ischaemic damage through permanent right common carotid ligation followed by hypoxia ( $8\%\ \text{O}_2$ ) (Figure 4a). A total of 60 animals were included in the study, randomly distributed in 5 treatment groups of 12. The histological damage evaluation shows that hypoxic-ischaemia induced a severe damage in the brain hemisphere ipsilateral to the occluded carotid (Figure 4b); in the vehicle-treated group, the whole hemisphere showed a volume reduction compared to contralateral hemisphere. Treatment with  $4\ \mu\text{g kg}^{-1}$  CHF6467, given 10 min after the damage, did not affect brain loss (Figure 4b). After administration of  $20\ \mu\text{g kg}^{-1}$  of CHF6467, there was a significant decrease in brain damage compared to vehicle-treated group both at 10 min, 1 h and 3 h after brain insult (Figure 4b). Coronal brain sections at the hippocampal level of a representative animal for each experimental group are shown in Figure 4c. Thus, at the intranasal dose of  $20\ \mu\text{g kg}^{-1}$



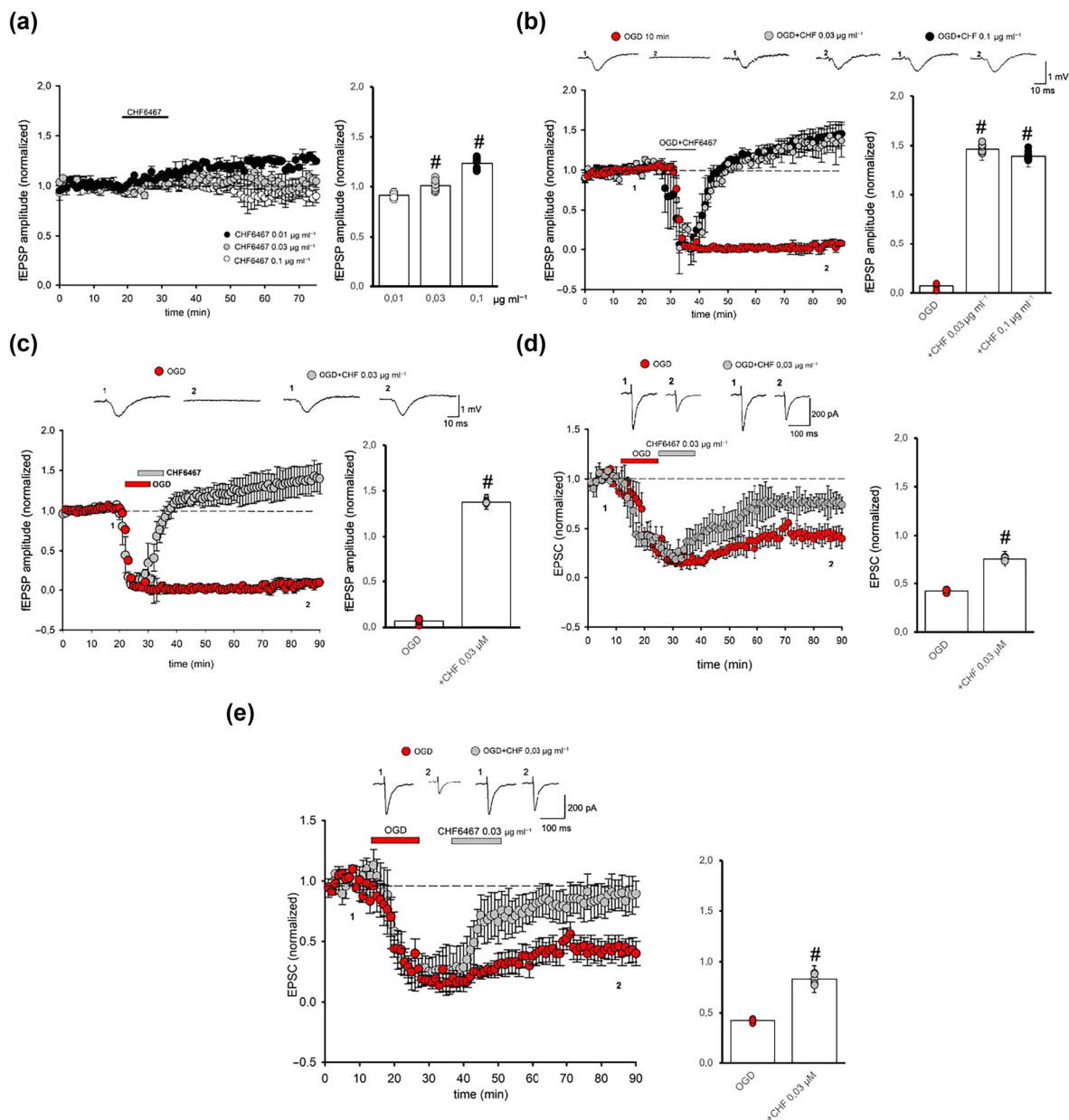


**FIGURE 2** CHF6467 reverted depression induced by oxygen and glucose deprivation (OGD) in hippocampal slices. (a) Superimposed pooled data showing fEPSP in slices treated with CHF6467 (15 min) at different concentration ( $0.01\text{--}0.1 \mu\text{g ml}^{-1}$ ). Histograms illustrate the amplitude of fEPSP. Data ( $n = 5$ ) are expressed as mean  $\pm$  SEM; # indicates significant differences between CHF6467  $0.01$  and  $0.1 \mu\text{g ml}^{-1}$  concentrations by unpaired Student's *t* test. (b) Superimposed pooled data showing fEPSP in slices treated with OGD (10 min), CHF6467  $0.03 \mu\text{g ml}^{-1}$  + OGD or CHF6467  $0.1 \mu\text{g ml}^{-1}$  + OGD. On top, representative traces for different conditions are shown. Histograms illustrate the amplitude of fEPSP in the different experimental conditions. Data ( $n = 5$ ) are expressed as mean  $\pm$  SEM; # indicates significant differences between CHF6467 + OGD and OGD treatment by an unpaired Student's *t* test. (c) Superimposed pooled data showing fEPSP in slices treated with OGD (10 min) or CHF6467  $0.03 \mu\text{g ml}^{-1}$  + OGD. On top, representative traces for different conditions are shown. Histograms illustrate the amplitude of fEPSP in both experimental conditions. Data ( $n = 5$ ) are expressed as mean  $\pm$  SEM; # indicates significant differences between CHF6467 + OGD and OGD treatment by unpaired Student's *t* test. (d) Superimposed pooled data showing EPSP in slices treated with OGD or CHF6467 + OGD, on top, representative traces for different experimental conditions are shown. Histograms illustrate the amplitude of EPSP. Data are expressed as mean  $\pm$  SEM; # indicates significant differences between two treatments by unpaired Student's *t* test. (e) Superimposed pooled data showing EPSP in slices treated with OGD (10 min) or CHF6467  $0.03 \mu\text{g ml}^{-1}$  after OGD. On top, representative traces for different experimental conditions are shown. Histograms illustrate the amplitude of fEPSP in both experimental conditions. Data ( $n = 5$ ) are expressed as mean  $\pm$  SEM; # indicates significant differences between CHF6467 after OGD and OGD treatment by an unpaired Student's *t* test.

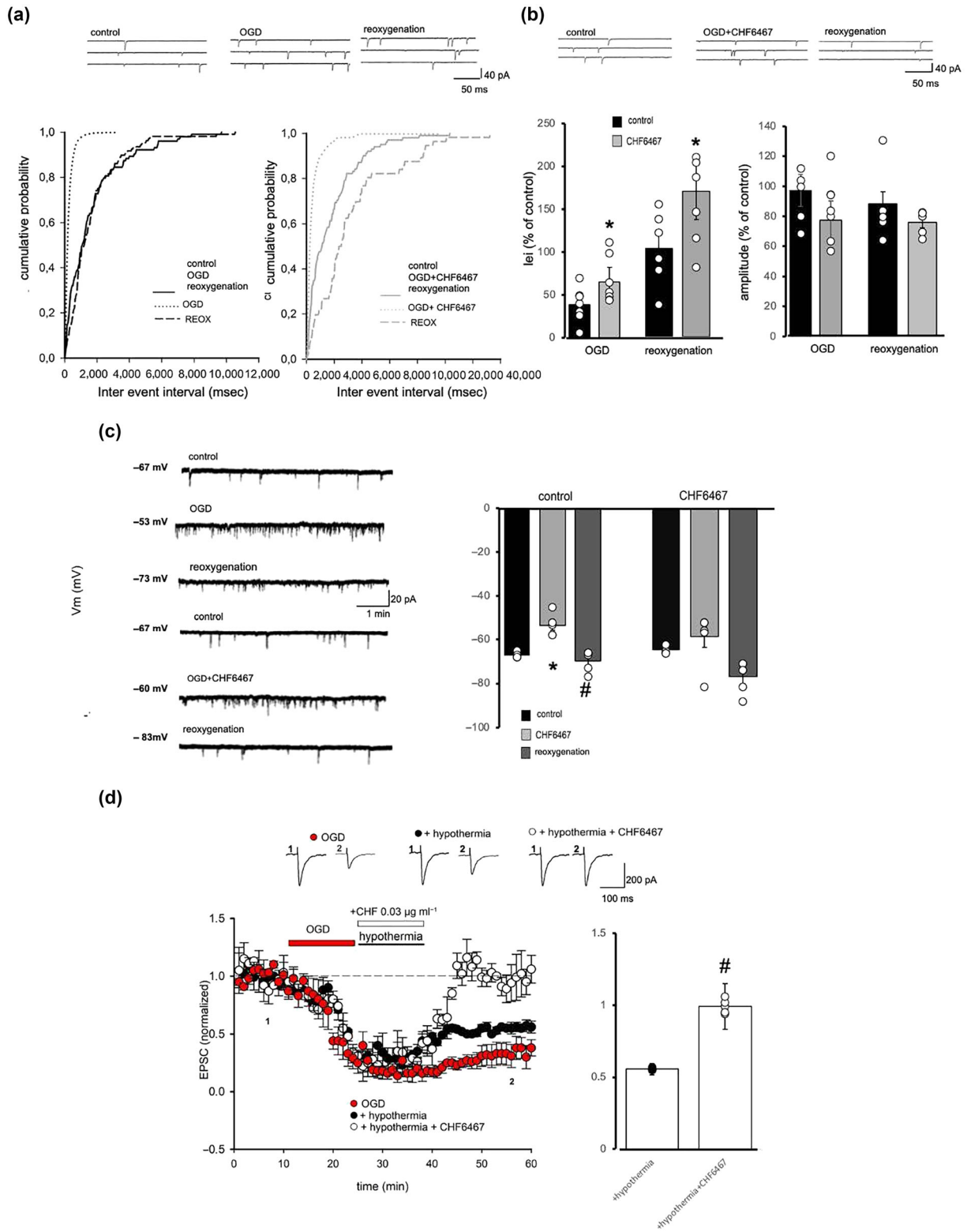


FIGURE 3 Legend on next page.

**FIGURE 3** Neuroprotective effect of CHF6467 on alterations induced by energy deprivation on pyramidal neuron and combined effect with hypothermia. (a) Pooled cumulative distributions of sEPSC inter event interval (bin size 50 ms) recorded from neurons in response to oxygen and glucose deprivation (OGD), CHF6467 + OGD and reoxygenation. On top, representative traces from different experimental conditions are shown. (b) Histograms show the effect of different treatments on inter event interval and amplitude of sEPSC (as % of control). Data ( $n = 5$ ) are expressed as mean  $\pm$  SEM; asterisk (\*) indicates significant differences between CHF6467 and control in different experimental conditions by an unpaired Student's *t* test. (c) On the left, representative traces from different experimental conditions are shown, histograms show the effect of CHF6467 treatment in different experimental conditions. Data ( $n = 5$ ) are expressed as mean  $\pm$  SEM; asterisk (\*) and # indicate significant differences by a paired Student's *t* test. (d) Superimposed pooled data showing EPSP in slices treated with OGD, OGD + hypothermia or OGD + CHF6467 + hypothermia. On top, representative traces for different experimental conditions are shown. Histograms illustrate the amplitude of EPSP. Data ( $n = 5$ ) are expressed as mean  $\pm$  SEM; # indicates significant differences between two treatments by an unpaired Student's *t* test. *ie*, inter-event interval.

dose, CHF6467 showed a significant neuroprotection up to 3 h after the hypoxic–ischaemic damage.

### 3.5 | CHF6467 reduces brain infarct volume and synergistically potentiates neuroprotection by hypothermia in experimental neonatal rat hypoxic–ischaemic encephalopathy (HIE)

In a second set of experiments conducted at University of Florence, Italy, we evaluated the neuroprotective effects of the combination of intranasal CHF6467 and TH in neonatal Wistar rats undergoing hypoxic–ischaemic damage through permanent left common carotid artery occlusion followed by hypoxia (Figure 5a). A total of 82 animals were enrolled. CHF6467 ( $20 \mu\text{g kg}^{-1}$ ) was given alone or in combination with hypothermia ( $32^\circ\text{C}$  for 4 h beginning 1 h after the end of hypoxia). Hypothermia significantly reduced the extension of the lesion when compared to vehicle-treated animals maintained in normothermia (Figure 5b). Similarly, CHF6467 significantly inhibited brain infarcted volume compared to vehicle (Figure 5b). Interestingly, CHF6467 in combination with hypothermia showed a dramatic reduction of brain lesion compared to both vehicle in normothermia and CHF6467 alone (Figure 5b). The potentiation of the hypothermia neuroprotective effect exerted by CHF6467 appears to be synergistic as shown by the significant positive interaction of the two fixed factors (CHF6467 and hypothermia) in a two-way ANOVA model applied on log-transformed brain infarcted volumes. Rostral to caudal coronal brain sections, staining with TCC, of representative animals for each experimental group are shown in Figure 5c. These data suggest that CHF6467 and hypothermia exert their neuroprotective activity non redundantly, likely acting on different biological pathways.

### 3.6 | CHF6467 attenuates brain mRNA cytokine elevations in experimental neonatal rat hypoxic–ischaemic encephalopathy (HIE)

To start dissecting the mechanisms associated with the neuroprotective activity shown by CHF6467, we measured cytokine mRNA expression in the hippocampus and frontoparietal cortex in a subset of neonatal HIE Wistar rats killed at 24 hours after the hypoxic–ischaemic insult. In both hippocampus and frontoparietal cortex, a

marked increase of mRNA levels of several cytokines and chemokines was observed in comparison with sham-operated controls (Figure 6a,b). CHF6467 ( $20 \mu\text{g kg}^{-1}$  i.n.) administered immediately after hypoxia significantly counteracted the upregulation of several neuroinflammatory markers (monocyte chemoattractant protein-1 [ccl2], chemokine [C-X-C motif] ligand 2 [cxcl2], TNF- $\alpha$ , interleukin-6 [IL-6], chemokine CC motif ligand 7 [ccl7] and chemokine ligand 20 [ccl20]) in the hippocampal region of rats subjected to the hypoxic–ischaemic insult while hypothermia alone was not as effective as CHF6467 (Figure 6a). The combination of hypothermia and CHF6467 did not differ significantly from the effect of CHF6467 alone (Figure 6a). In the cortex, intranasal CHF6467 alone counteracted upregulation of some neuroinflammatory markers (but only chemokine (C-X-C motif) ligand 2, cxcl2, reached a statistical significance) induced by the hypoxic–ischaemic insult and such effect was, for some neuroinflammatory markers (ccl7, ccl2, IL-6 and TNF- $\alpha$ ), augmented by the combination with hypothermia (Figure 6b).

### 3.7 | CHF6467 attenuates long-term behavioural deficits and synergistically potentiates neuroprotection by hypothermia in experimental neonatal rat hypoxic–ischaemic encephalopathy (HIE)

The neuroprotective effects of intranasal CHF6467 ( $20 \mu\text{g kg}^{-1}$ ) were tested in experimental HIE alone or in combination with hypothermia, and the impact on long-term behavioural deficits was evaluated. CHF6467 was administered by the intranasal route immediately and 24, 48 and 72 h after the end of hypoxia at the dose of  $20 \mu\text{g kg}^{-1}$  that was shown to be well tolerated in previous experiments. All pups were then maintained with their dams, and they were subjected to behavioural tests at PND 60 before killing (Figure 7a). A total of 110 rats were enrolled, with 6 rats dying during the surgery and one animal dying 8 days after ischaemia. The animals were randomly assigned to five groups: 23 rats undergoing sham lesion, 21 rats undergoing hypoxic–ischaemic insult, 20 rats undergoing hypoxic–ischaemic insult and receiving CHF6467, 19 rats undergoing hypoxic–ischaemic insult plus hypothermia, and 20 rats undergoing hypoxic–ischaemic insult and CHF6467 plus hypothermia. The left eye (ipsilateral to the ischaemic insult) opening day was delayed in hypoxic–ischaemic animals versus sham, and we observed a significant improvement of eye opening in

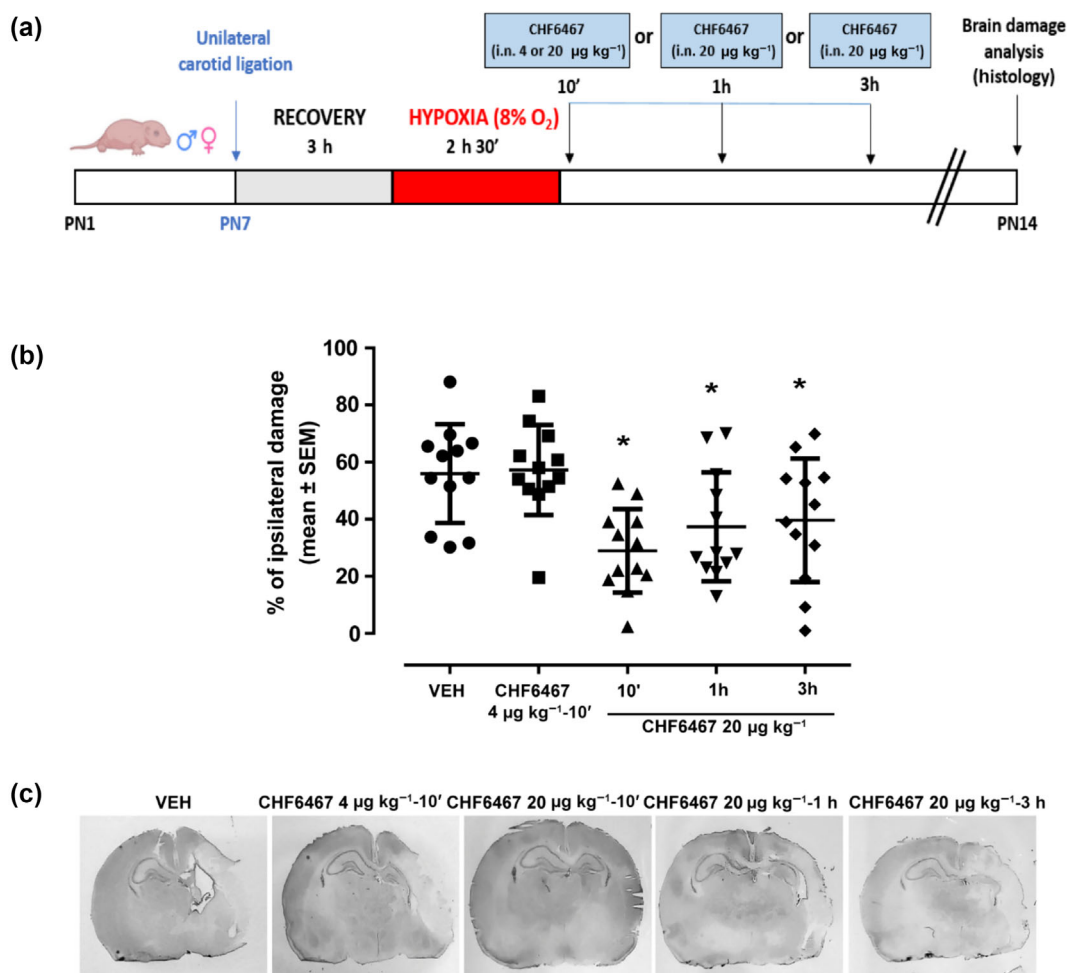


**FIGURE 4** Effects of intranasal CHF6467 doses and time of administration on brain infarct volume in experimental neonatal rat hypoxic-ischaemic encephalopathy (HIE). (a) Diagram of the experimental study protocol. (b) Brain infarct volume calculated for the whole hemisphere. CHF6467 was administered at the single dose of 4 μg kg<sup>-1</sup> 10 min after brain damage (CHF6467 4 μg, 10') or at the single dose of 20 μg kg<sup>-1</sup> 10 min, 1 h or 3 h after brain insult. Results are expressed as percent of ipsilateral damage calculated from bilateral regional volumes using the following formula:  $100(L-R)/L$  where L is left-side volume (contralateral) and R is right-side volume (ipsilateral). Data are expressed as mean ± SEM. n = 12/group; \*P < 0.05 versus vehicle (VEH)-treated group. The effects of the 20 μg kg<sup>-1</sup> 10', 1 h and 3 h after the brain damage were compared to that of the vehicle group with one-way ANOVA followed by the Holm-Sidak procedure for multiple comparison versus the control group (VEH-treated animals). (c) Coronal brain sections at the hippocampal level of a representative animal for each experimental group

animals treated with hypothermia or CHF6467 alone or in combination versus hypoxic-ischaemic animals (data not shown). At PND 60, lesioned animals who received vehicle showed high number of falls and limited motility on Rotarod with latency that was significantly increased by both CHF6467 and hypothermia. The combination of CHF6467 and hypothermia significantly reduced the number of falls and extended the latency compared to normothermia alone (Figure 7b,c). At PND 60, memory performance in animals treated with hypothermia or CHF6467 significantly improved compared to vehicle-treated lesioned animals both on the Y-maze (discrimination index, Figure 7d) and the novel object recognition (percent alternation, Figure 7e) tests. Memory performance of animals treated with the combination of CHF6467 plus TH approached that of sham animals on both tests. We have observed that CHF6467 and TH are neuroprotective per se and showed synergic effects when they are administered in combination to HIE rats (TTC staining 72 h after the end of

hypoxia, Figure 5b). In Figure 7f-h, by measuring infarct volume by toluidine staining analysis, we showed that the magnitude of such neuroprotective effect is still evident 53 days after the end of hypoxia. These data combined with behavioural data demonstrate that the neuroprotective effect of CHF6467 persists over time.

### 3.8 | Intranasal CHF6467 combined with therapeutic hypothermia (TH) attenuates the elevation of plasma neurofilament light chain (NfL) levels induced by hypoxic-ischaemic encephalopathy (HIE)

We then verified if the central neuroprotective activity of intranasal CHF6467 could be detected peripherally by measuring plasma levels of neurofilament light chain (NfL), a marker of neuro-axonal damage that is becoming very popular in clinical studies (Mullard, 2023). We

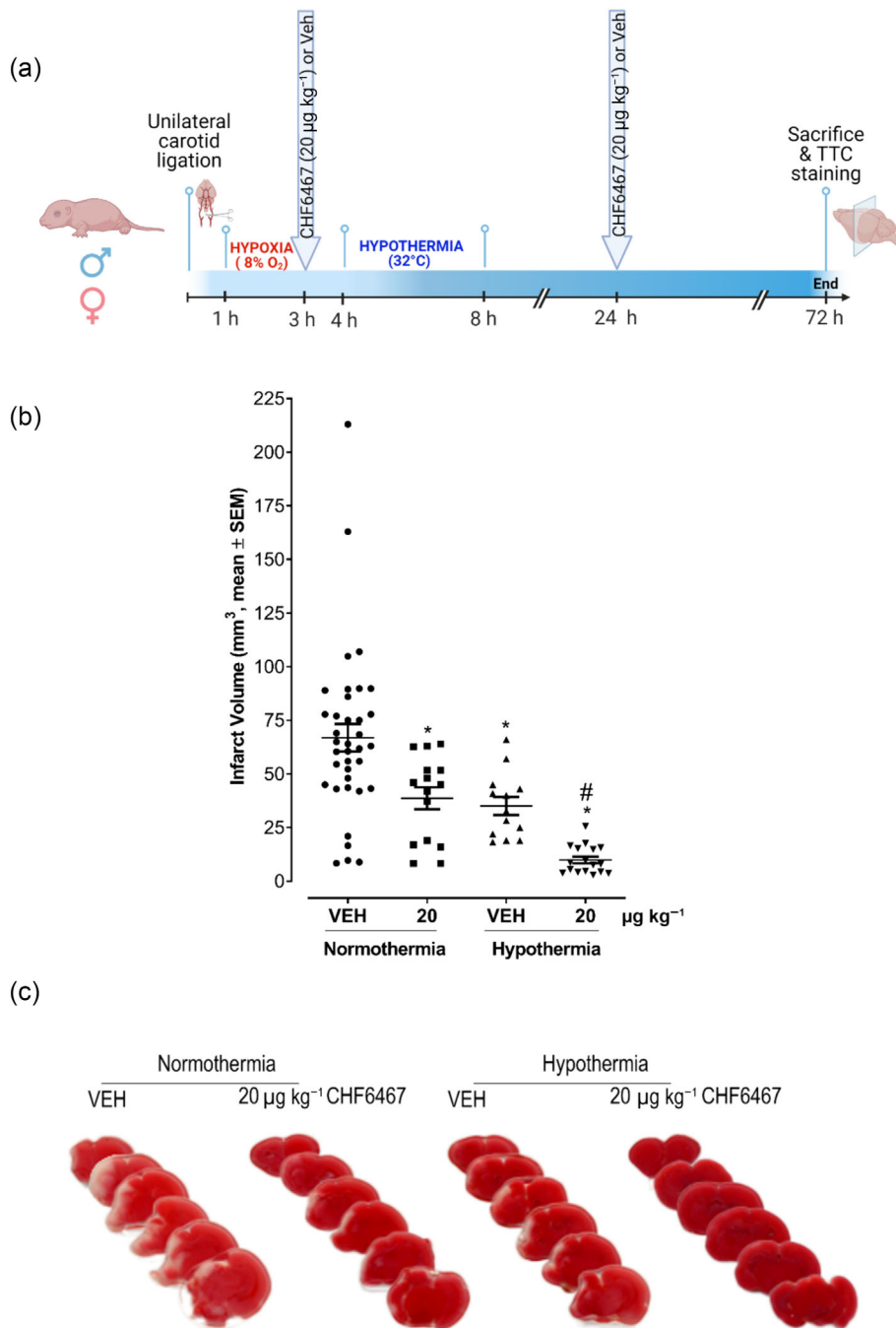


**FIGURE 5** Intranasal CHF6467 alone or in combination with therapeutic hypothermia is neuroprotective in experimental neonatal rat hypoxic–ischaemic encephalopathy (HIE).

(a) Diagram of the experimental protocol. Post-natal day (PND) 7 rat pups were subjected to left carotid artery occlusion followed by exposure to 2 h of hypoxia. CHF6467 was intranasally delivered at the dose of  $20 \mu\text{g kg}^{-1}$  ( $4 \mu\text{l}$  total volume,  $2 \mu\text{l}$  per nostril), alternating nostrils with an interval of 2 min between doses immediately (0 h) and 24 h after the end of hypoxia. Hypothermia ( $32^\circ\text{C}$  for 4 h) was applied starting 1 h after the end of hypoxia. (b) Quantitative analysis showing that CHF6467 ( $20 \mu\text{g kg}^{-1}$ ) and hypothermia significantly reduced the infarct volume induced by HIE. CHF6467 plus hypothermia showed greater neuroprotection than CHF6467 or hypothermia alone. Vehicle (VEH) normothermia ( $n = 37$ ); CHF6467 ( $20 \mu\text{g kg}^{-1}$ ) normothermia ( $n = 15$ ); VEH hypothermia ( $n = 13$ ); CHF6467 ( $20 \mu\text{g kg}^{-1}$ ) hypothermia ( $n = 17$ )  $*P < 0.05$  versus VEH normothermia;  $\#P < 0.05$  versus HIE +  $20 \mu\text{g kg}^{-1}$  CHF6467 at normothermia (one-way ANOVA + Tukey's *w* test). (c) Rostral to caudal coronal brain sections of representative animals for each experimental group are shown.

used again the experimental paradigm (neonatal Wistar rats undergoing hypoxic–ischaemic damage) in which we observed the highest neuroprotective activity (72 h after the end of hypoxia, by TTC staining) when intranasal CHF6467 was combined with TH. In this experiment, we used a higher dose of CHF6467 ( $40 \mu\text{g kg}^{-1}$ ) either per se and in combination with TH to extend the dose range tested. Quantitative and qualitative analysis confirmed that CHF6467 at  $40 \mu\text{g kg}^{-1}$ , similarly to the lower dose of  $20 \mu\text{g kg}^{-1}$ , significantly reduced the infarct volume induced by HIE (Figure 8a,b) and CHF6467 plus TH showed greater neuroprotection than CHF6467 or TH alone (Figure 8a,b). In a subset of animals, blood was collected at killing (72 h after the insult), and NfL was measured.

Significantly higher levels of NfL were detected in HIE animals compared to unlesioned animals. Both CHF6467 and TH treatments showed a tendency in decreasing plasma NfL levels, while their combination significantly lowered NfL in plasma (Figure 8c).

### 3.9 | Intranasal CHF6467 reaches the brain at biologically active concentrations

Mass spectrometry was used to specifically detect and quantify CHF6467 in brain homogenates as described in the supporting information (Figure S1). We first tested the distribution of CHF6467 after

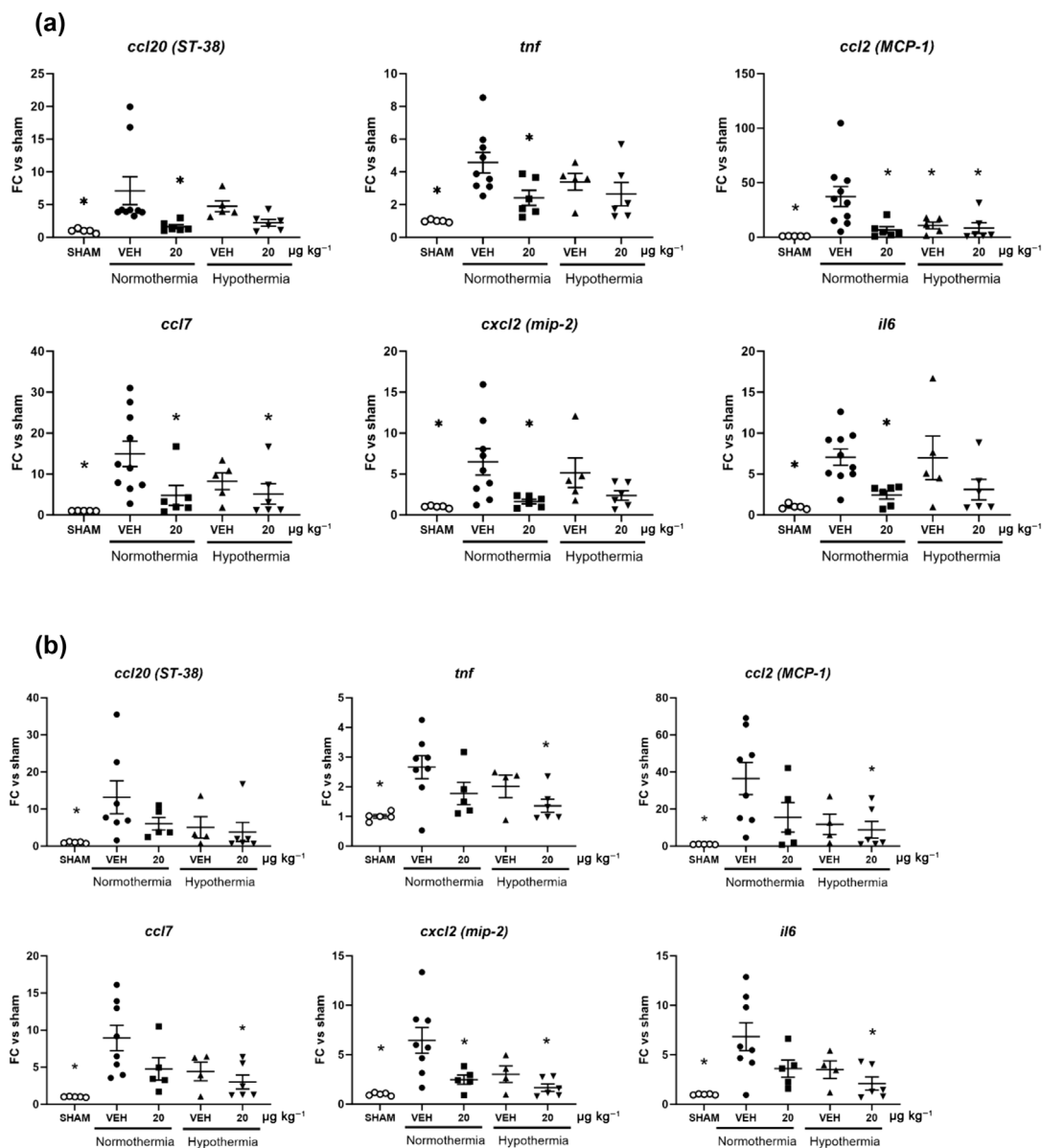


**FIGURE 6** Effects of CHF6467 alone or in combination with therapeutic hypothermia on brain mRNA cytokine levels in experimental neonatal rat hypoxic-ischaemic encephalopathy (HIE). (a) Hippocampal mRNA levels of a panel of rat cytokines and chemokines in sham-operated, vehicle-treated HIE, HIE treated with CHF6467, 20 µg kg<sup>-1</sup>, HIE treated with therapeutic hypothermia, HIE treated with CHF6467 and hypothermia. Scatter plots with means ± SEM. \*P < 0.05 versus vehicle (VEH) normothermia. (b) Cortical mRNA levels of a panel of rat cytokines and chemokines in sham-operated (n = 5); hypoxic-ischaemic encephalopathy (HIE) (n = 8); HIE treated with CHF6467, 20 µg kg<sup>-1</sup> (n = 5); HIE treated with hypothermia (n = 4); and HIE treated with CHF6467 and hypothermia (n = 6). Scatter plots with means ± SEM. \*P < 0.05 versus VEH normothermia (one-way ANOVA + Dunnett's test). FC,

intranasal administration (40 µg kg<sup>-1</sup>) in control neonatal PND7 rats. This proof of principle was performed on a small number of samples: three olfactory bulbs, two hippocampi and two cerebral cortexes. CHF6467 was detected in all the samples, providing further evidence of its ability to reach the brain areas of interest upon intranasal administration. Quantification estimates, performed based on SSSHPIFHR peptide signals (Figure S2), showed that, on average, a few hundred of picograms can be found in the cortical areas and in the hippocampi.

## 4 | DISCUSSION

In this manuscript, we described a wide set of in vitro and in vivo experiments evaluating the neuroprotective effects of CHF6467 against hypoxic-ischaemic brain damage. CHF6467 was tested in different experimental in vitro and in vivo rodent models. We provided multiple converging evidences obtained at two different research sites independently that CHF6467 administered intranasally after the induction of the hypoxic ischaemic insult reduces brain damage in two

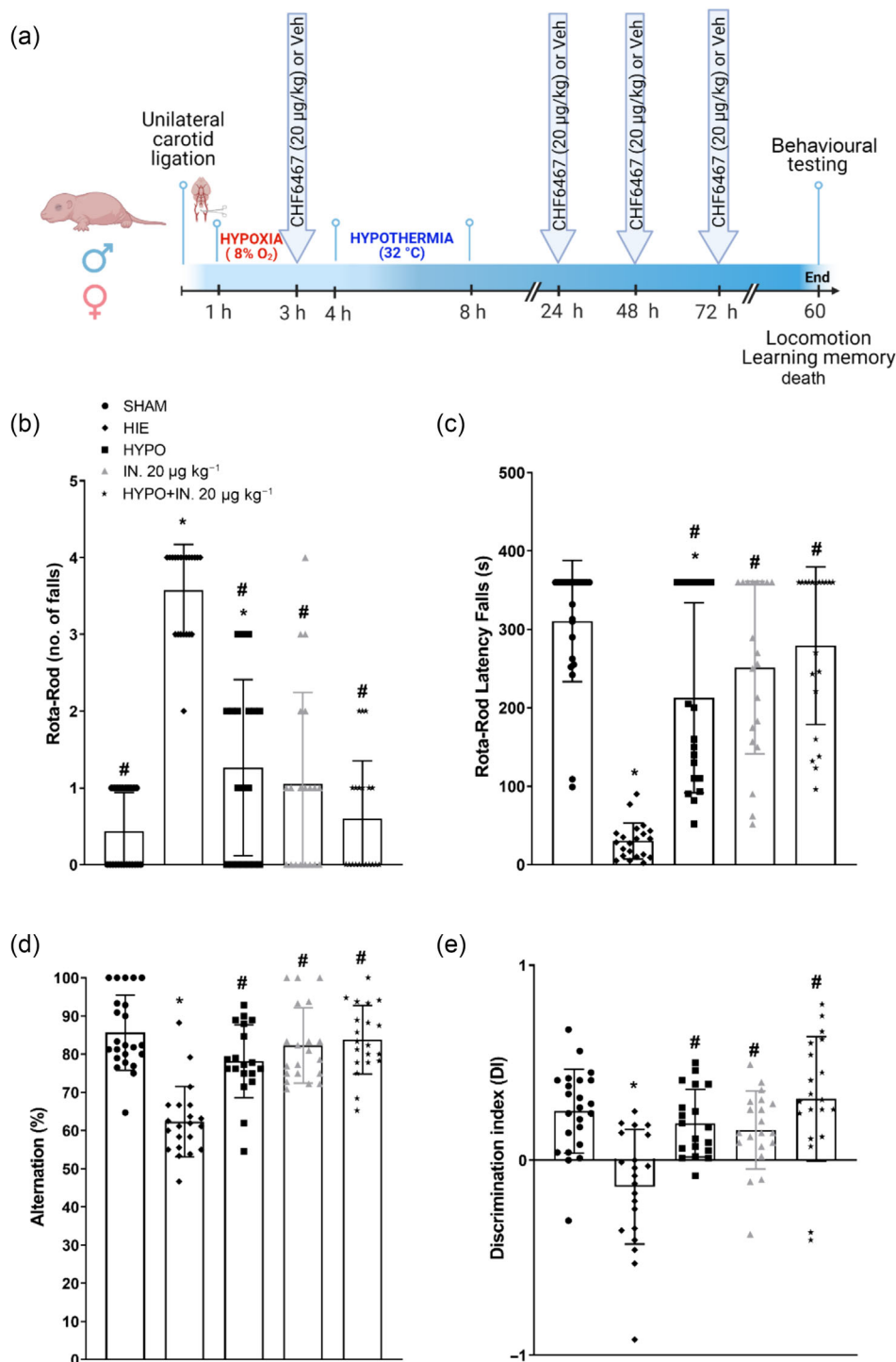


**FIGURE 7** Intranasal CHF6467 alone or in combination with therapeutic hypothermia attenuates long-term behavioural deficits in experimental neonatal rat hypoxic–ischaemic encephalopathy (HIE). (a) Schematic representation of the experimental protocol of the behavioural study. (b, c) CHF6467 alone or in combination with hypothermia improves the HIE-induced locomotion impairment in the Rota-rod test. (d) CHF6467 alone or in combination with TH improves the HIE-induced memory impairment in the Y-maze test. (e) CHF6467 alone or in combination with hypothermia improves the HIE-induced cognitive impairment in the novel object recognition test. Data are expressed as individual data points for each animal and bars represent means  $\pm$  SEM (b–e). \* $P < 0.05$  vs. SHAM; # $P < 0.05$  versus HIE (one-way ANOVA + Tukey's *w* test). (f) CHF6467 alone or in combination with therapeutic hypothermia (TH) reduces ischaemic area and volume (g) of rats exposed to HIE at 60 PND as shown also by representative images (h). SHAM ( $n = 23$ ) vehicle (VEH) normothermia ( $n = 21$ ); CHF6467 ( $20 \mu\text{g kg}^{-1}$ ) normothermia ( $n = 20$ ); VEH hypothermia ( $n = 19$ ); CHF6467 ( $20 \mu\text{g kg}^{-1}$ ) hypothermia ( $n = 20$ ). Data are expressed as individual data points for each animal and bars represent means  $\pm$  SEM (f, g). \* $P < 0.05$ , versus VEH normothermia (one-way ANOVA + Tukey's *w* test)

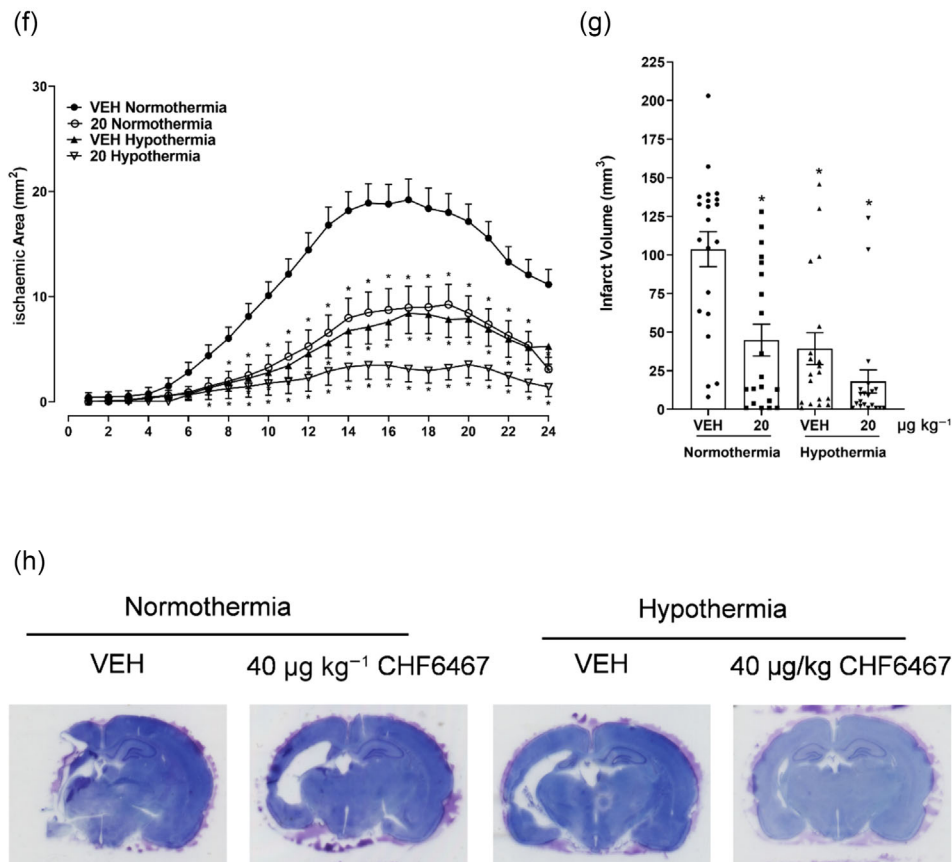


FIGURE 7 (Continued)

different strains of neonatal rats. We initially investigated different doses of CHF6467 to define an optimal neuroprotective dose. Results revealed a significant reduction of brain damage when CHF6467 was intranasally administered during the early phase of brain damage development. Furthermore, we determined a time window of intervention for CHF6467 by showing that its protective effect was still significant when administered 3 h following the insult. As TH is already a routine therapy for neonatal encephalopathy, we also demonstrated that intranasal CHF6467, in combination with TH, attenuated or even reversed long-term motor coordination and memory deficit of neonatal rats subjected to hypoxic-ischaemic insult. The neuroprotective effect (reduction of the infarct volume) of the combination of CHF6467 (20 and 40 μg kg<sup>-1</sup>) and TH was larger than the sum of the individual effects of CHF6467 and TH suggesting a synergistic interaction between the two treatments. Electrophysiological studies complement these *in vivo* findings by demonstrating that the neuroprotective effects of CHF6467 *in vitro* were dramatically enhanced by TH up to an almost complete reversal of neuronal electrophysiological damage. Measurements in plasma of NfL, a widely accepted biomarker of neuronal damage in humans (Mullard, 2023), reflected the neuroprotective effects of CHF6467 in combination with TH, and could represent an important surrogate marker to assess the neuroprotective activity of CHF6467 in future clinical studies. Gene expression measurements suggest that the protective effects of CHF6467 are associated with

the counteracting of neuroinflammatory marker upregulation induced by hypoxic-ischaemic insult. It is increasingly recognized that one of the leading pathogenic factors of neonatal brain damage is inflammation, induced by activation of the central and peripheral immune systems (Hagberg et al., 2015). Neuroinflammatory responses are induced within minutes and can expand for weeks and even months after the insult (Fleiss et al., 2015). Indeed, our experimental data show that CHF6467 blunted the upregulation of cytokine expression in brain samples of neonatal rats subjected to hypoxic-ischaemic damage. Although we cannot exclude that such an effect is secondary to the mitigation of the insult, there is evidence suggesting that NGF attenuates pro-inflammatory responses in microglia and may thereby contribute to regulation of neuroinflammation (Fodelianaki et al., 2019). Moreover, CHF6467 proved to be more potent than NGF in reducing the pro-inflammatory markers of human microglia polarization (Lisi et al., 2022). Thus, one possible mode of action of CHF6467 is blunting neuroinflammation associated with hypoxic-ischaemic brain insult and such an effect is additive when combined with TH.

The intranasal route has also been successfully used for NGF in animal models of traumatic brain injury (Lv et al., 2013; Manni, Conti, et al., 2023; Tian et al., 2012). Encouraging clinical case reports employing intranasal NGF have been described in children with brain injury (Chiaretti et al., 2017; Curatola et al., 2023; Gatto et al., 2023) and in an infant with bacterial meningitis (Chiaretti et al., 2020). We



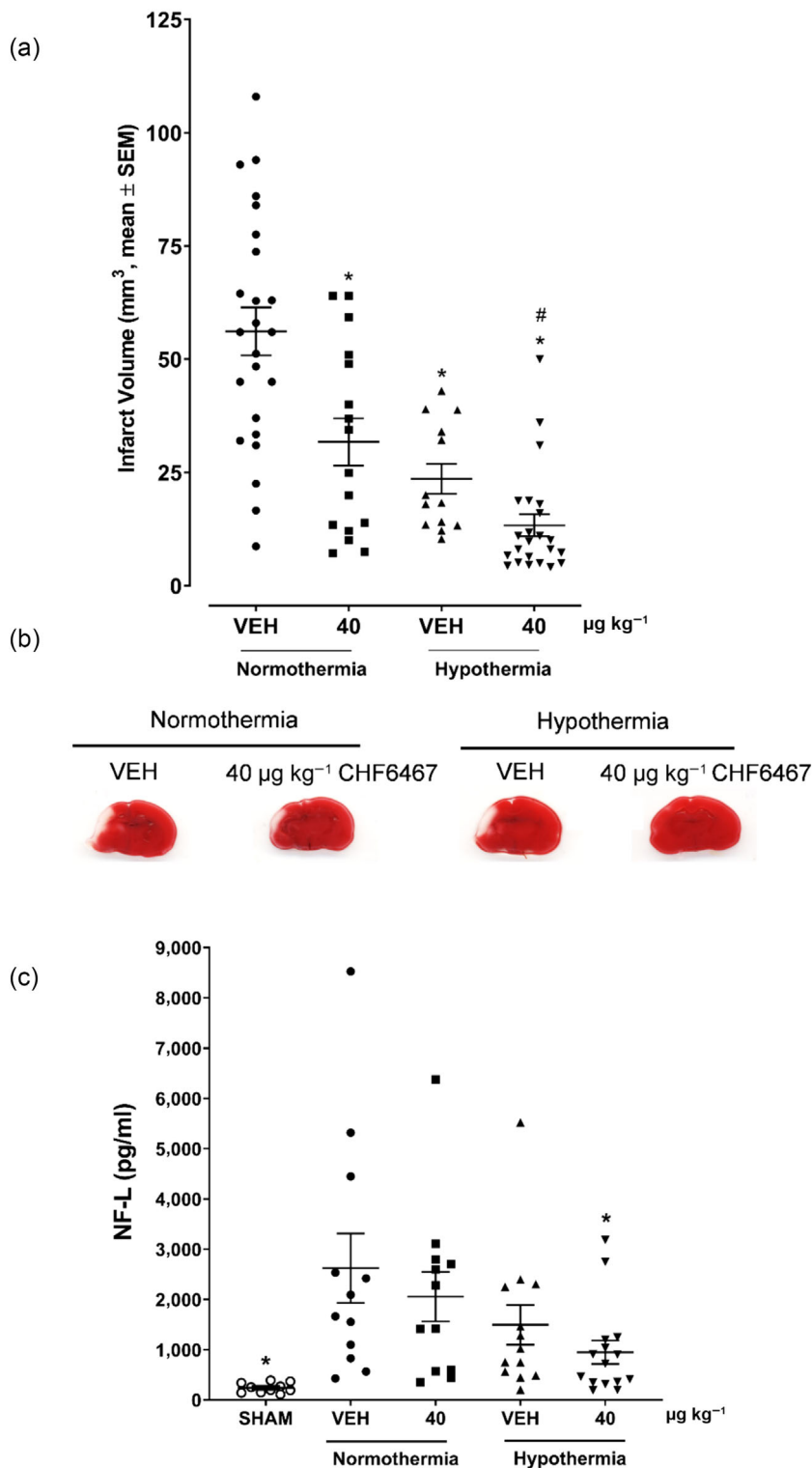


**FIGURE 8** Effects of CHF6467 alone or in combination with therapeutic hypothermia on infarct volume and plasma neurofilament light chain (NfL) levels in experimental neonatal rat HIE. (a) Quantitative analysis showing that CHF6467 (40 µg kg<sup>-1</sup>) and hypothermia significantly reduced the infarct volume induced by hypoxic-ischaemic encephalopathy (HIE). CHF6467 plus hypothermia showed greater neuroprotection than CHF6467 or hypothermia alone. \**P* < 0.05 versus vehicle (VEH) normothermia; #*P* < .05 versus HIE + 40 µg kg<sup>-1</sup> CHF6467 at normothermia (one-way ANOVA + Tukey's *w* test). VEH normothermia (*n* = 24); CHF6467 (40 µg kg<sup>-1</sup>) normothermia (*n* = 16); VEH hypothermia (*n* = 13); CHF6467 (40 µg kg<sup>-1</sup>) hypothermia (*n* = 23). (b) Representative qualitative images of brain coronal sections. (c) Plasma NfL levels in lesioned neonatal rats treated with vehicle, hypothermia, CHF6467 (40 µg kg<sup>-1</sup>) alone or in combination with hypothermia. Mean NfL levels in the CHF6467 plus hypothermia were significantly lower than those in lesioned rats treated with vehicle. Plasma samples were collected at post-natal day 10, three days after the insult. NfL plasma levels were measured with an ELISA kit. \**P* < 0.05 versus VEH normothermia (one-way ANOVA + Dunnett's test). SHAM (*n* = 10); VEH normothermia (*n* = 12); CHF6467 (40 µg kg<sup>-1</sup>) normothermia (*n* = 12); VEH hypothermia (*n* = 13); CHF6467 (40 µg kg<sup>-1</sup>) hypothermia (*n* = 15)

conducted mass spectrometry analyses showing that CHF6467 reaches different regions of the brain after intranasal administration in neonatal rodents, adding further evidence to the feasibility of this route of administration (supporting information).

Although highly encouraging, the present study has some limitations. We did not investigate the effect of CHF6467 on repair processes, specific cellular subpopulations and the vascular niche, nor did we fully establish the mechanism underlying functional recovery and

reduction of brain damage (Hatayama et al., 2022). Moreover, we did not test CHF6467 in experimental models based on larger gyrencephalic animals, such as sheep or piglets, that may better mimic the human brain and nasal cavities anatomy (Landucci et al., 2022). On the other hand, conducting such experiments in larger species, considering the need for an adequate sample size, poses logistical and ethical challenges that deserve to be tackled in a dedicated study. Finally, since measurements of cytokines and chemokines mRNA expression

were done without perfusing animals, the results may be affected by residual blood remaining in brain vessels.

In conclusion, we showed that CHF6467 is neuroprotective in different *in vitro* hypoxic–ischaemic encephalopathy (HIE) hippocampal slice subjected to oxygen–glucose deprivation and that intranasal CHF6467 reduces brain hypoxic–ischaemic damage and improves behavioural outcomes in experimental HIE. Moreover, intranasal CHF6467 reduces brain infarct volume in experimental HIE more effectively when combined with TH and attenuates neurobehavioural deficits, brain neuroinflammatory markers and a serum marker of neuroaxonal damage. Although further safety/toxicological studies are needed to progress to clinical studies, the present results highlight the relevance of CHF6467 as a new promising therapeutic agent for the treatment of neonatal HIE.

## AUTHOR CONTRIBUTIONS

**E. Landucci:** Conceptualization (equal); data curation (lead); formal analysis (lead); investigation (equal); methodology (lead); validation (lead); visualization (lead); writing—original draft (lead). **D. Mango:** Data curation (equal); formal analysis (equal); investigation (equal); methodology (equal); writing—original draft (equal). **S. Carloni:** Data curation (equal); formal analysis (equal); investigation (equal); methodology (equal); writing—original draft (supporting). **C. Mazzantini:** Data curation (equal); investigation (equal); methodology (equal). **D. E. Pellegrini-Giampietro:** Supervision (equal). **A. Saidi:** Investigation (equal); methodology (equal). **W. Balduini:** Supervision (equal). **E. Schiavi:** Data curation (equal); formal analysis (equal); methodology (equal); visualization (equal); writing—original draft (supporting). **L. Tigli:** Data curation (equal); methodology (equal). **B. Pioselli:** Data curation (equal); methodology (equal). **B. P. Imbimbo:** Conceptualization (equal); formal analysis (equal); funding acquisition (lead); project administration (equal); supervision (equal); writing—original draft (equal). **F. Facchinetti:** Conceptualization (lead); funding acquisition (equal); project administration (equal); supervision (lead); visualization (equal); writing—original draft (lead).

## ACKNOWLEDGEMENT

We would like to thank Stefano Vezzoli for statistical support. This study was supported by Chiesi Farmaceutici S.p.A., Parma, Italy.

## CONFLICT OF INTEREST STATEMENT

ES, LT, BP, FF and BPI are employees at Chiesi Farmaceutici S.p.A. that do not hold Chiesi Farmaceutici S.p.A. stocks or equity shares. The other authors have no competing interest to declare.

## DATA AVAILABILITY STATEMENT

The data that support the findings of this study are available from the corresponding author upon reasonable request.

## DECLARATION OF TRANSPARENCY AND SCIENTIFIC RIGOUR

This declaration acknowledges that this paper adheres to the principles for transparent reporting and scientific rigour of preclinical

research as stated in the BJP guidelines for Design and Analysis, Immunoblotting and Immunochemistry and Animal Experimentation and as recommended by funding agencies, publishers and other organizations engaged with supporting research.

## ORCID

Fabrizio Facchinetti  <https://orcid.org/0000-0003-3505-4159>

## REFERENCES

- Alexander, S. P. H., Fabbro, D., Kelly, E., Mathie, A. A., Peters, J. A., Veale, E. L., Armstrong, J. F., Faccenda, E., Harding, S. D., Davies, J. A., Beuve, A., Brouckaert, P., Bryant, C., Burnett, J. C., Farndale, R. W., Friebe, A., Garthwaite, J., Hobbs, A. J., Jarvis, G. E., ... Waldman, S. A. (2023). The Concise Guide to PHARMACOLOGY 2023/24: Catalytic receptors. *British Journal of Pharmacology*, 180, S241–S288. <https://doi.org/10.1111/bph.16180>
- Apfel, S. C., Kessler, J. A., Adornato, B. T., Litchy, W. J., Sanders, C., & Rask, C. A. (1998). Recombinant human nerve growth factor in the treatment of diabetic polyneuropathy. NGF study group. *Neurology*, 51, 695–702. <https://doi.org/10.1212/WNL.51.3.695>
- Armogida, M., Spalloni, A., Amantea, D., Nutini, M., Petrelli, F., Longone, P., Bagetta, G., Nisticò, R., & Mercuri, N. B. (2011). The protective role of catalase against cerebral ischemia *in vitro* and *in vivo*. *International Journal of Immunopathology and Pharmacology*, 24, 735–747. <https://doi.org/10.1177/039463201102400320>
- Brust, V., Schindler, P. M., & Lewejohann, L. (2015). Lifetime development of behavioural phenotype in the house mouse (*Mus musculus*). *Frontiers in Zoology*, 12, S17. <https://doi.org/10.1186/1742-9994-12-S1-S17>
- Capsoni, S., Covaceuszach, S., Marinelli, S., Ceci, M., Bernardo, A., Minghetti, L., Ugolini, G., Pavone, F., & Cattaneo, A. (2011). Taking pain out of NGF: A “painless” NGF mutant, linked to hereditary sensory autonomic neuropathy type V, with full neurotrophic activity. *PLoS ONE*, 6, e17321. <https://doi.org/10.1371/journal.pone.0017321>
- Capsoni, S., Malerba, F., Carucci, N. M., Rizzi, C., Criscuolo, C., Origlia, N., Calvella, M., Viegi, A., Meli, G., & Cattaneo, A. (2017). The chemokine CXCL12 mediates the anti-amyloidogenic action of painless human nerve growth factor. *Brain*, 140, 201–217. <https://doi.org/10.1093/brain/aww271>
- Castillo, J., Dávalos, A., Naveiro, J., & Noya, M. (1996). Neuroexcitatory amino acids and their relation to infarct size and neurological deficit in ischemic stroke. *Stroke*, 27, 1060–1065. <https://doi.org/10.1161/01.STR.27.6.1060>
- Chen, X. F., Wu, Y., Kim, B., Nguyen, K. V., Chen, A., Qiu, J., Santoso, A. R., Disdier, C., Lim, Y. P., & Stonestreet, B. S. (2024). Neuroprotective efficacy of hypothermia and inter-alpha inhibitor proteins after hypoxic ischemic brain injury in neonatal rats. *Neurotherapeutics*, e00341. <https://doi.org/10.1016/j.neurot.2024.e00341>
- Chiaretti, A., Conti, G., Falsini, B., Buonsenso, D., Crasti, M., Manni, L., Soligo, M., Fantacci, C., Genovese, O., Calcagni, M. L., di Giuda, D., Mattoli, M. V., Cocciolillo, F., Ferrara, P., Ruggiero, A., Staccioli, S., Colafati, G. S., & Riccardi, R. (2017). Intranasal nerve growth factor administration improves cerebral functions in a child with severe traumatic brain injury: A case report. *Brain Injury*, 31, 1538–1547. <https://doi.org/10.1080/02699052.2017.1376760>
- Chiaretti, A., Eftimiadi, G., Buonsenso, D., Rendeli, C., Staccioli, S., & Conti, G. (2020). Intranasal nerve growth factor administration improves neurological outcome after GBS meningitis. *Child's Nervous System*, 36, 2083–2088. <https://doi.org/10.1007/s00381-020-04590-x>
- Clarkson, J. M., Martin, J. E., & McKeegan, D. E. F. (2022). A review of methods used to kill laboratory rodents: Issues and opportunities. *Laboratory Animals*, 56, 419–436. <https://doi.org/10.1177/00236772221097472>

- Covaceuszach, S., Capsoni, S., Marinelli, S., Pavone, F., Ceci, M., Ugolini, G., Vignone, D., Amato, G., Paoletti, F., Lamba, D., & Cattaneo, A. (2010). In vitro receptor binding properties of a 'painless' NGF mutein, linked to hereditary sensory autonomic neuropathy type V. *Biochemical and Biophysical Research Communications*, 391, 824–829. <https://doi.org/10.1016/j.bbrc.2009.11.146>
- Curatola, A., Graglia, B., Granata, G., Conti, G., Capossela, L., Manni, L., Ferretti, S., di Giuda, D., Romeo, D. M., Calcagni, M. L., Soligo, M., Castelli, E., Piastra, M., Mantelli, F., Marca, G. D., Staccioli, S., Romeo, T., Pani, M., Cocciolillo, F., ... Chiaretti, A. (2023). Combined treatment of nerve growth factor and transcranial direct current stimulations to improve outcome in children with vegetative state after out-of-hospital cardiac arrest. *Biology Direct*, 18, 24. <https://doi.org/10.1186/s13062-023-00379-5>
- Curtis, M. J., Alexander, S. P. H., Cirino, G., George, C. H., Kendall, D. A., Insel, P. A., Izzo, A. A., Ji, Y., Panettieri, R. A., Patel, H. H., Sobey, C. G., Stanford, S. C., Stanley, P., Stefanska, B., Stephens, G. J., Teixeira, M. M., Vergnolle, N., & Ahluwalia, A. (2022). Planning experiments: Updated guidance on experimental design and analysis and their reporting III. *British Journal of Pharmacology*, 179, 3907–3913. <https://doi.org/10.1111/bph.15868>
- Dingley, J., Tooley, J., Porter, H., & Thoresen, M. (2006). Xenon provides short-term neuroprotection in neonatal rats when administered after hypoxia-ischemia. *Stroke*, 37, 501–506. <https://doi.org/10.1161/01.STR.0000198867.31134.ac>
- Fleiss, B., Tann, C. J., Degos, V., Sigaut, S., van Steenwinckel, J., Schang, A. L., Kichev, A., Robertson, N. J., Mallard, C., Hagberg, H., & Gressens, P. (2015). Inflammation-induced sensitization of the brain in term infants. *Developmental Medicine and Child Neurology*, 57(Suppl 3), 17–28. <https://doi.org/10.1111/dmcn.12723>
- Fodelianaki, G., Lansing, F., Bhattarai, P., Troullinaki, M., Zeballos, M. A., Charalampopoulos, I., Gravanis, A., Mirtschink, P., Chavakis, T., & Alexaki, V. I. (2019). Nerve growth factor modulates LPS-induced microglial glycolysis and inflammatory responses. *Experimental Cell Research*, 377, 10–16. <https://doi.org/10.1016/j.yexcr.2019.02.023>
- Gatto, A., Capossela, L., Conti, G., Eftimiadi, G., Ferretti, S., Manni, L., Curatola, A., Graglia, B., di Sarno, L., Calcagni, M. L., di Giuda, D., Cecere, S., Romeo, D. M., Soligo, M., Picconi, E., Piastra, M., della Marca, G., Staccioli, S., Ruggiero, A., ... Chiaretti, A. (2023). Intranasal human-recombinant NGF administration improves outcome in children with post-traumatic unresponsive wakefulness syndrome. *Biology Direct*, 18, 61. <https://doi.org/10.1186/s13062-023-00418-1>
- Gerace, E., Landucci, E., Scartabelli, T., Moroni, F., & Pellegrini-Giampietro, D. E. (2012). Rat hippocampal slice culture models for the evaluation of neuroprotective agents. *In Methods in Molecular Biology*, 846, 343–354. [https://doi.org/10.1007/978-1-61779-536-7\\_29](https://doi.org/10.1007/978-1-61779-536-7_29)
- Hagberg, H., Mallard, C., Ferriero, D. M., Vannucci, S. J., Levison, S. W., Vexler, Z. S., & Gressens, P. (2015). The role of inflammation in perinatal brain injury. *Nature Reviews. Neurology*, 11, 192–208. <https://doi.org/10.1038/nrneurol.2015.13>
- Hatayama, K., Riddick, S., Awa, F., Chen, X., Virgintino, D., & Stonestreet, B. (2022). Time course of changes in the neurovascular unit after hypoxic-ischemic injury in neonatal rats. *International Journal of Molecular Sciences*, 23, 4180. <https://doi.org/10.3390/ijms23084180>
- Holtzman, D. M., Kilbridge, J., Li, Y., Cunningham, E. T., Lenn, N. J., Clary, D. O., Reichardt, L. F., & Mobley, W. C. (1995). TrkA expression in the CNS: Evidence for the existence of several novel NGF-responsive CNS neurons. *The Journal of Neuroscience*, 15, 1567–1576. <https://doi.org/10.1523/JNEUROSCI.15-02-01567.1995>
- Holtzman, D. M., Sheldon, R. A., Jaffe, W., Cheng, Y., & Ferriero, D. M. (1996). Nerve growth factor protects the neonatal brain against hypoxic-ischemic injury. *Annals of Neurology*, 39, 114–122. <https://doi.org/10.1002/ana.410390117>
- Jönhagen, M. E., Nordberg, A., Amberla, K., Bäckman, L., Ebendal, T., Meyerson, B., Olson, L., Seiger, S. M., Theodorsson, E., Viitanen, M., Winblad, B., & Wahlund, L. O. (1998). Intracerebroventricular infusion of nerve growth factor in three patients with Alzheimer's disease. *Dementia and Geriatric Cognitive Disorders*, 9, 246–257. <https://doi.org/10.1159/000017069>
- Landucci, E., Filippi, L., Gerace, E., Catarzi, S., Guerrini, R., & Pellegrini-Giampietro, D. E. (2018). Neuroprotective effects of topiramate and memantine in combination with hypothermia in hypoxic-ischemic brain injury in vitro and in vivo. *Neuroscience Letters*, 668, 103–107. <https://doi.org/10.1016/j.neulet.2018.01.023>
- Landucci, E., Mazzantini, C., Lana, D., Davolio, P. L., Giovannini, M. G., & Pellegrini-Giampietro, D. E. (2021). Neuroprotective effects of cannabidiol but not  $\Delta^9$ -tetrahydrocannabinol in rat hippocampal slices exposed to oxygen-glucose deprivation: Studies with cannabis extracts and selected cannabinoids. *International Journal of Molecular Sciences*, 22, 9773. <https://doi.org/10.3390/ijms22189773>
- Landucci, E., Pellegrini-Giampietro, D. E., & Facchinetti, F. (2022). Experimental models for testing the efficacy of pharmacological treatments for neonatal hypoxic-ischemic encephalopathy. *Biomedicine*, 10, 937.
- Landucci, E., Scartabelli, T., Gerace, E., Moroni, F., & Pellegrini-Giampietro, D. E. (2011). CB1 receptors and post-ischemic brain damage: Studies on the toxic and neuroprotective effects of cannabinoids in rat organotypic hippocampal slices. *Neuropharmacology*, 60, 674–682. <https://doi.org/10.1016/j.neuropharm.2010.11.021>
- Li, X., Li, F., Ling, L., Li, C., & Zhong, Y. (2018). Intranasal administration of nerve growth factor promotes angiogenesis via activation of PI3K/Akt signaling following cerebral infarction in rats. *American Journal of Translational Research*, 10, 3481–3492.
- Lilley, E., Stanford, S. C., Kendall, D. E., Alexander, S. P. H., Cirino, G., Docherty, J. R., George, C. H., Insel, P. A., Izzo, A. A., Ji, Y., Panettieri, R. A., Sobey, C. G., Stefanska, B., Stephens, G., Teixeira, M., & Ahluwalia, A. (2020). ARRIVE 2.0 and the British Journal of Pharmacology: Updated guidance for 2020. *British Journal of Pharmacology*, 177, 3611–3616. <https://doi.org/10.1111/bph.15178>
- Lisi, L., Marinelli, S., Ciotti, G. M. P., Pizzoferrato, M., Palmerio, F., Chiavari, M., Cattaneo, A., & Navarra, P. (2022). The effects of painless nerve growth factor on human microglia polarization. *Frontiers in Cellular Neuroscience*, 16, 969058. <https://doi.org/10.3389/fncel.2022.969058>
- Lorenzini, L., Baldassarro, V. A., Stanzani, A., & Giardino, L. (2021). Nerve growth factor: The first molecule of the neurotrophin family. *Advances in Experimental Medicine and Biology*, 1331, 3–10. [https://doi.org/10.1007/978-3-030-74046-7\\_1](https://doi.org/10.1007/978-3-030-74046-7_1)
- Lv, Q., Fan, X., Xu, G., Liu, Q., Tian, L., Cai, X., Sun, W., Wang, X., Cai, Q., Bao, Y., Zhou, L., Zhang, Y., Ge, L., Guo, R., & Liu, X. (2013). Intranasal delivery of nerve growth factor attenuates aquaporins-4-induced edema following traumatic brain injury in rats. *Brain Research*, 1493, 80–89. <https://doi.org/10.1016/j.brainres.2012.11.028>
- Malerba, F., Paoletti, F., Bruni Ercole, B., Materazzi, S., Nassini, R., Coppi, E., Patacchini, R., Capsoni, S., Lamba, D., & Cattaneo, A. (2015). Functional characterization of human ProNGF and NGF mutants: Identification of NGF P61SR100E as a "painless" lead investigational candidate for therapeutic applications. *PLoS ONE*, 10, e0136425. <https://doi.org/10.1371/journal.pone.0136425>
- Mango, D., & Nisticò, R. (2019). Acid-sensing ion channel 1a is involved in N-methyl D-aspartate receptor-dependent long-term depression in the hippocampus. *Frontiers in Pharmacology*, 10, 555. <https://doi.org/10.3389/fphar.2019.00555>
- Manni, L., Conti, G., Chiaretti, A., & Soligo, M. (2021). Intranasal delivery of nerve growth factor in neurodegenerative diseases and Neurotrauma. *Frontiers in Pharmacology*, 12, 754502. <https://doi.org/10.3389/fphar.2021.754502>
- Manni, L., Conti, G., Chiaretti, A., & Soligo, M. (2023). Intranasal nerve growth factor for prevention and recovery of the outcomes of

- traumatic brain injury. *Neural Regeneration Research*, 18, 773–778. <https://doi.org/10.4103/1673-5374.354513>
- Manni, L., Leotta, E., Mollica, I., Serafino, A., Pignataro, A., Salvatori, I., Conti, G., Chiaretti, A., & Soligo, M. (2023). Acute intranasal treatment with nerve growth factor limits the onset of traumatic brain injury in young rats. *British Journal of Pharmacology*, 180, 1949–1964. <https://doi.org/10.1111/bph.16056>
- Millar, L. J., Shi, L., Hoerder-Suabedissen, A., & Molnár, Z. (2017). Neonatal hypoxia ischaemia: Mechanisms, models, and therapeutic challenges. *Frontiers in Cellular Neuroscience*, 11, 78. <https://doi.org/10.3389/fncel.2017.00078>
- Minnone, G., de Benedetti, F., & Bracci-Laudiero, L. (2017). NGF and its receptors in the regulation of inflammatory response. *International Journal of Molecular Sciences*, 18, 1028. <https://doi.org/10.3390/ijms18051028>
- Mullard, A. (2023). NFL makes regulatory debut as neurodegenerative disease biomarker. *Nature Reviews. Drug Discovery*, 22, 431–434. <https://doi.org/10.1038/d41573-023-00083-z>
- Öz, P., & Saybaşlı, H. (2017). In vitro detection of oxygen and glucose deprivation-induced neurodegeneration and pharmacological neuroprotection based on hippocampal stratum pyramidale width. *Neuroscience Letters*, 636, 196–204. <https://doi.org/10.1016/j.neulet.2016.11.027>
- Patel, S. D., Pierce, L., Ciardiello, A. J., & Vannucci, S. J. (2014). Neonatal encephalopathy: Pre-clinical studies in neuroprotection. *Biochemical Society Transactions*, 42, 564–568. <https://doi.org/10.1042/BST20130247>
- Percie du Sert, N., Hurst, V., Ahluwalia, A., Alam, S., Avey, M. T., Baker, M., Browne, W. J., Clark, A., Cuthill, I. C., Dirnagl, U., Emerson, M., Garner, P., Holgate, S. T., Howells, D. W., Karp, N. A., Lazic, S. E., Lidster, K., MacCallum, C. J., Macleod, M., ... Würbel, H. (2020). The ARRIVE guidelines 2.0: Updated guidelines for reporting animal research. *BMJ Open Science*, 4, e100115.
- Pöyhönen, S., Er, S., Domanskyi, A., & Airavaara, M. (2019). Effects of neurotrophic factors in glial cells in the central nervous system: Expression and properties in neurodegeneration and injury. *Frontiers in Physiology*, 10, 486. <https://doi.org/10.3389/fphys.2019.00486>
- Sabir, H., Scull-Brown, E., Liu, X., & Thoresen, M. (2012). Immediate hypothermia is not neuroprotective after severe hypoxia-ischemia and is deleterious when delayed by 12 hours in neonatal rats. *Stroke*, 43, 3364–3370. <https://doi.org/10.1161/STROKEAHA.112.674481>
- Severini, C., Petrocchi Passeri, P., Ciotti, M. T., Florenzano, F., Petrella, C., Malerba, F., Bruni, B., D'Onofrio, M., Arisi, I., Brandi, R., Possenti, R., Calissano, P., & Cattaneo, A. (2017). Nerve growth factor derivative NGF61/100 promotes outgrowth of primary sensory neurons with reduced signs of nociceptive sensitization. *Neuropharmacology*, 117, 134–148. <https://doi.org/10.1016/j.neuropharm.2017.01.035>
- Testa, G., Mainardi, M., Morelli, C., Olimpico, F., Pancrazi, L., Petrella, C., Severini, C., Florio, R., Malerba, F., Stefanov, A., Strettoi, E., Brandi, R., Arisi, I., Heppenstall, P., Costa, M., Capsoni, S., & Cattaneo, A. (2019). The TaNGFR100W mutation specifically impairs nociception without affecting cognitive performance in a mouse model of hereditary sensory and autonomic neuropathy type V. *The Journal of Neuroscience*, 39, 9702–9715. <https://doi.org/10.1523/JNEUROSCI.0688-19.2019>
- Tian, L., Guo, R., Yue, X., Lv, Q., Ye, X., Wang, Z., Chen, Z., Wu, B., Xu, G., & Liu, X. (2012). Intranasal administration of nerve growth factor ameliorate  $\beta$ -amyloid deposition after traumatic brain injury in rats. *Brain Research*, 1440, 47–55. <https://doi.org/10.1016/j.brainres.2011.12.059>
- Vogel-Ciernia, A., & Wood, M. A. (2014). Examining object location and object recognition memory in mice. *Current Protocols in Neuroscience*, 69, 8.31.1–17.
- Wise, B. L., Seidel, M. F., & Lane, N. E. (2021). The evolution of nerve growth factor inhibition in clinical medicine. *Nature Reviews Rheumatology*, 17, 34–46. <https://doi.org/10.1038/s41584-020-00528-4>

## SUPPORTING INFORMATION

Additional supporting information can be found online in the Supporting Information section at the end of this article.

**How to cite this article:** Landucci, E., Mango, D., Carloni, S., Mazzantini, C., Pellegrini-Giampietro, D. E., Saidi, A., Balduini, W., Schiavi, E., Tigli, L., Pioselli, B., Imbimbo, B. P., & Facchinetti, F. (2025). Beneficial effects of CHF6467, a modified human nerve growth factor, in experimental neonatal hypoxic–ischaemic encephalopathy. *British Journal of Pharmacology*, 182(3), 510–529. <https://doi.org/10.1111/bph.17353>